



3 4456 0050603 0

Cy 1

Uranium Dispersion in the Coating of Weak-Acid-Resin-Derived HTGR Fuel Microspheres

G. W. Weber
R. L. Seatty
V. J. Tennery
W. J. Lackey, Jr.

OAK RIDGE NATIONAL LABORATORY
CENTRAL RESEARCH LIBRARY
DOCUMENT COLLECTION

LIBRARY LOAN COPY

DO NOT TRANSFER TO ANOTHER PERSON

If you wish someone else to see this document, send in name with document and the library will arrange a loan.

UCRL-7968
23 3-472

OAK RIDGE NATIONAL LABORATORY

OPERATED BY UNION CARBIDE CORPORATION FOR THE ENERGY RESEARCH AND DEVELOPMENT ADMINISTRATION

Printed in the United States of America. Available from
National Technical Information Service
U.S. Department of Commerce
5285 Port Royal Road, Springfield, Virginia 22161
Price: Printed Copy \$5.50; Microfiche \$2.25

This report was prepared as an account of work sponsored by the United States Government. Neither the United States nor the Energy Research and Development Administration, nor any of their employees, nor any of their contractors, subcontractors, or their employees, makes any warranty, express or implied, or assumes any legal liability or responsibility for the accuracy, completeness or usefulness of any information, apparatus, product or process disclosed, or represents that its use would not infringe privately owned rights.

ORNL/TM-5133
UC-77 -- Gas-Cooled
Reactor Technology

Contract No. W-7405-eng-26

METALS AND CERAMICS DIVISION

URANIUM DISPERSION IN THE COATING OF WEAK-ACID-RESIN-DERIVED
HTGR FUEL MICROSPHERES

G. W. Weber, R. L. Beatty, V. J. Tennery,
and W. J. Lackey, Jr.

FEBRUARY 1976

OAK RIDGE NATIONAL LABORATORY
Oak Ridge, Tennessee 37830
operated by
UNION CARBIDE CORPORATION
for the
U.S. ENERGY RESEARCH AND DEVELOPMENT ADMINISTRATION



3 4456 0050603 0

CONTENTS

ABSTRACT	1
INTRODUCTION	2
DESCRIPTION OF FUEL FABRICATION AND COATING	2
POSSIBLE CAUSES OF DISPERSION.	9
CLASSIFICATION OF DISPERSION TYPES	9
EXPERIMENTS AND RESULTS	11
Effect of $UC_{1-x}O_x$ Phase on Fuel Dispersion	11
Effect of Air and/or Moisture Exposure on Fuel Dispersion	13
Effect of Chlorine Contamination on Fuel Dispersion	18
Chlorine Introduction During Coating	19
Permeation of the LTI Coating by Chlorine During SiC Deposition	19
Mechanical Attrition	36
DISCUSSION OF RESULTS	36
CONCLUSIONS AND RECOMMENDATIONS	41
ACKNOWLEDGMENTS	41

URANIUM DISPERSION IN THE COATING OF WEAK-ACID-RESIN-DERIVED
HTGR FUEL MICROSPHERES

G. W. Weber, R. L. Beatty, V. J. Tennery,
and W. J. Lackey, Jr.

ABSTRACT

The current reference HTGR recycle fuel particle is a UO_2/UC_2 kernel with a Triso coating comprising a low-density pyrocarbon (PyC) buffer, a high-density PyC inner LTI coating, SiC, and a high-density PyC outer LTI. The kernel is fabricated from a weak-acid ion exchange resin (WAR).

Microradiographic examination of coated WAR particles has demonstrated that considerable uranium can be transferred from the kernel to the buffer coating during fabrication. Investigation of causes of fuel dispersion has indicated several different factors that contribute to fuel redistribution if not properly controlled. The presence of a nonequilibrium $UC_{1-x}O_x$ ($0 \leq x \leq 0.3$) phase, had no significant effect on initiating fuel dispersion. Gross exposure of the completed fuel kernel to ambient atmosphere or to water vapor at room temperature produced very minimal levels of dispersion. Exposure of the fuel to perchloroethylene (C_2Cl_4) during buffer and inner LTI deposition produced massive uranium redistribution. Perchloroethylene is used in a prototype coating furnace to scrub the off-gas and hence is a potential source of chlorine. The formation of a volatile uranium-containing chlorine species is the probable mechanism for fuel redistribution in this instance.

Fuel redistribution observed in Triso-coated particles results from permeation of the inner LTI by HCl during SiC deposition. As the decomposition of methyltrichlorosilane (CH_3Cl_3Si) is used to deposit SiC, chlorine is readily available during this process. The permeability of the inner LTI coating has a marked effect on the extent of this mode of fuel dispersion.

LTI permeability was determined by chlorine leaching studies to be a strong function of density, coating gas dilution, and coating temperature but relatively unaffected by application of a seal coat, variations in coating thickness, and annealing at 1800°C.

Mechanical attrition of the kernels during processing was identified as a potential source of uranium-bearing fines that may be incorporated into the coating in some circumstances.

INTRODUCTION

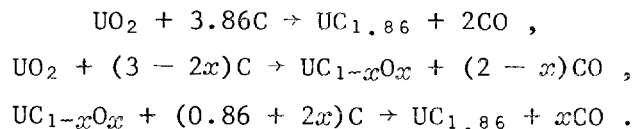
The reference high-temperature gas-cooled reactor (HTGR) fissile particle for fresh and recycle fuel is a Triso-coated kernel derived from weak-acid ion exchange resin (WAR). The kernel composition is nominally a controlled mixture of UO_2 , UC_2 , and $UC_{1-x}O_x$ ($0 \leq x \leq 0.3$) with excess carbon. The coating comprises in radial order from the fuel kernel, a low-density pyrolytic carbon (PyC) buffer, a high-density PyC, silicon carbide, and a second high-density PyC. Particles coated with the first two layers only are designated as Biso-coated. A contact microradiograph of qualified Biso-coated fuel is shown in Fig. 1. The white uranium-containing kernel and two coating layers are plainly delineated.

During recent processing of specimens for irradiation testing, however, heavy metal appeared in significant amounts in the buffer coating layer. Radiographs taken of material 75% converted to UC_2 after Biso coating and annealing, represented in Fig. 2, show concentrations of high x-ray absorption material, presumably uranium, in the buffer region of the coating. Figures 3, 4, and 5 give results of optical microscopy and electron microprobe examination of Biso-coated particles having three different oxygen levels (carbothermic conversion levels) following a 30 min anneal at $1800^\circ C$. These figures show that the dispersed material does, in fact, contain uranium and that the dispersion is more severe for higher conversion levels (lower fuel oxygen content).

Since one of the principal functions of the buffer coating is to protect the inner LTI pyrocarbon from fission fragment recoil, the present work was undertaken to determine the cause(s) of this behavior and to identify critical process parameters or controls that could be used to prevent such fuel dispersion.

DESCRIPTION OF FUEL FABRICATION AND COATING

Weak-acid resin fuel particles are fabricated by the processing steps shown in Fig. 6. Sized and shape-separated acrylic acid divinylbenzene copolymer is loaded with uranyl ions¹ and dried at approximately $110^\circ C$ to yield resin containing UO_2^{2+} with some remaining water. This material is then heated to $1200^\circ C$ in a fluidized-bed carbonization process, which removes any remaining water and destructively distills the resin. The resultant material is UO_2 dispersed in 4 to 6 moles of carbon per mole of uranium. Further thermal treatment involves heating at 1550 to $1800^\circ C$ to carbothermally reduce the UO_2 in a conversion process. Conversion proceeds by removal of the oxygen by the reactions



¹P. A. Haas, *Loading a Cation Exchange Resin with Uranyl Ions* U.S. Patent 3,800,023 (March 26, 1974).

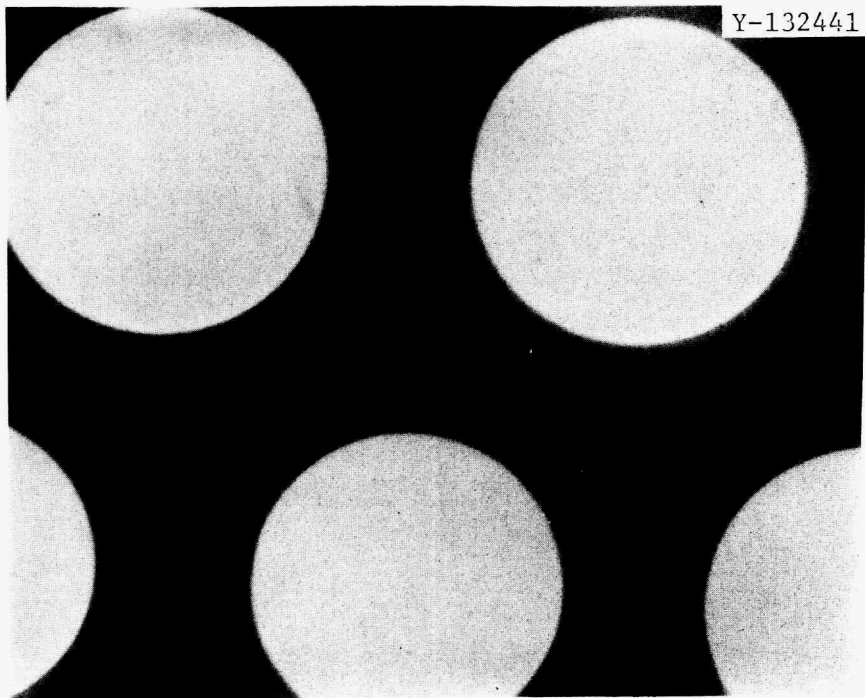


Fig. 1. Radiograph of 60%-Converted Biso-Coated Weak-Acid Resin Fuel with Typical Behavior. Batch OR-2359 HT 2. 100 \times .

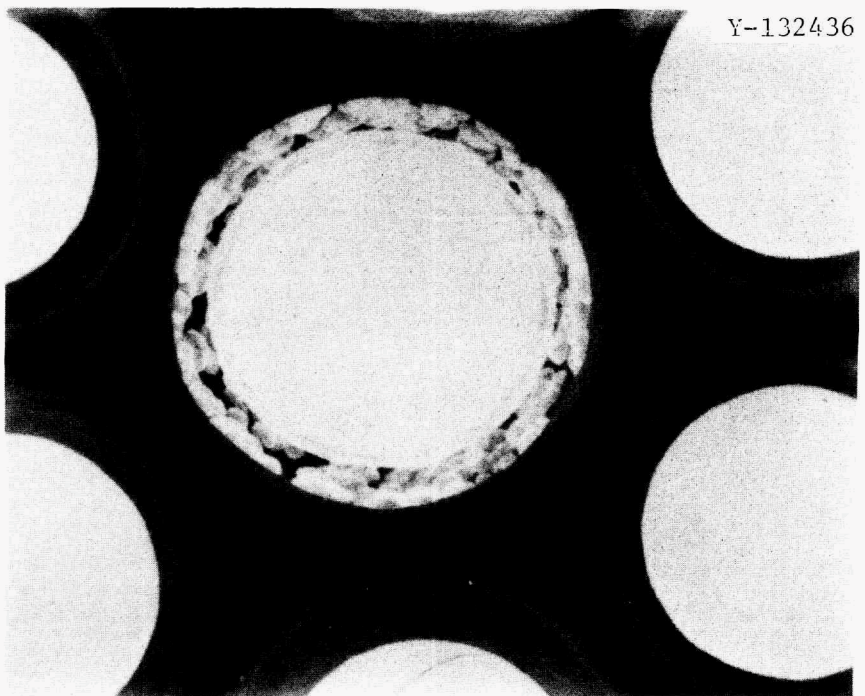


Fig. 2. Uranium Dispersion in 75%-Converted Biso-Coated WAR Fuel. (A-608). 100 \times .

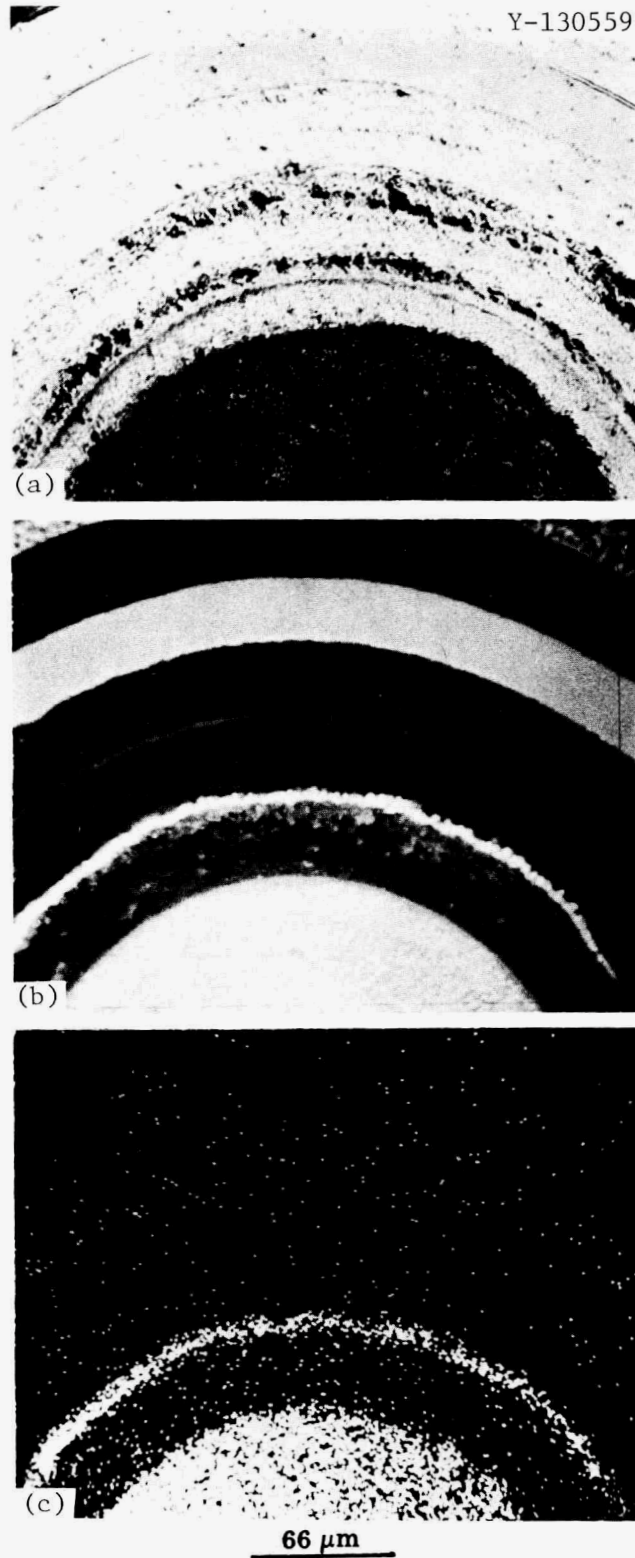


Fig. 3. Uranium Distribution in Coated, Carbonized, and Converted Weak-Acid Resin Microspheres. Batch A-601, 69.4%-converted. (a) Optical micrograph. (b) Backscattered electron image. (c) U $M\alpha$ x-ray image.

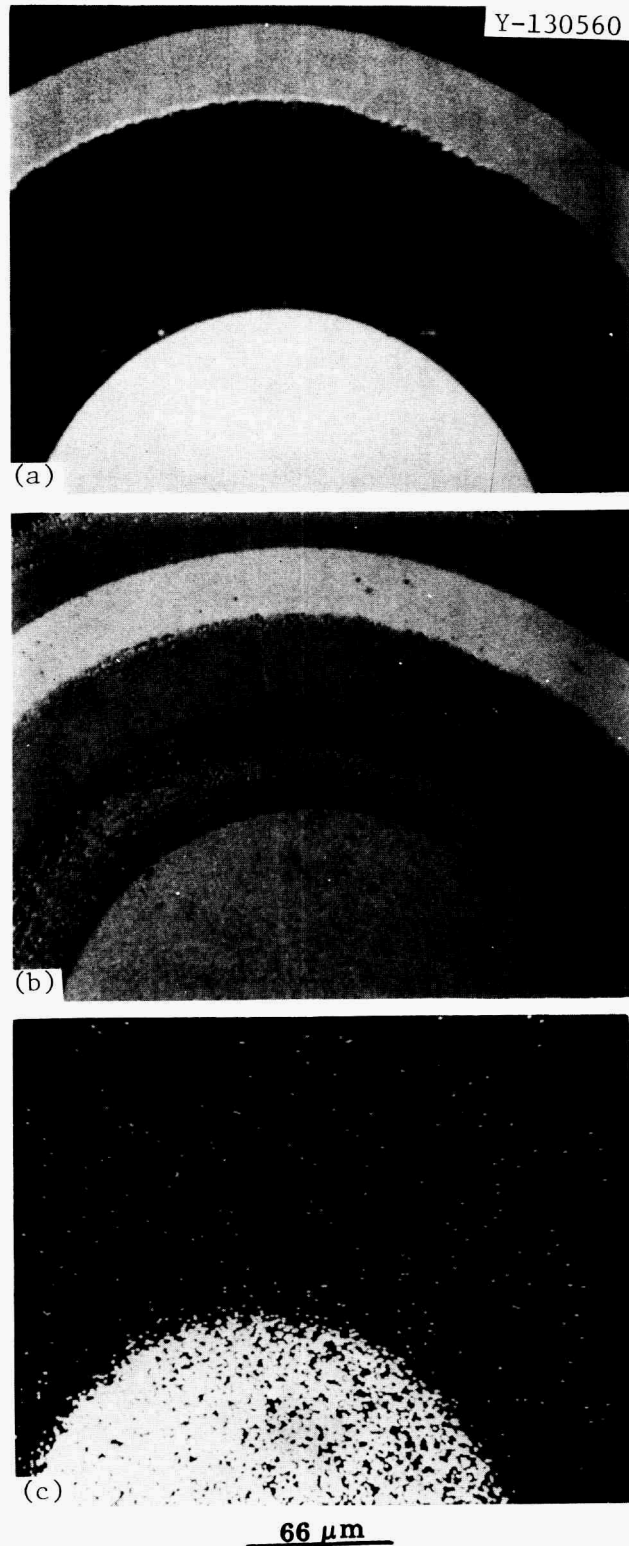


Fig. 4. Uranium Distribution in Coated, Carbonized, and Converted Weak-Acid Resin Microspheres. Batch A-611, 12.6%-converted. (a) Optical micrograph. (b) Backscattered electron image. (c) U $M\alpha$ x-ray image.

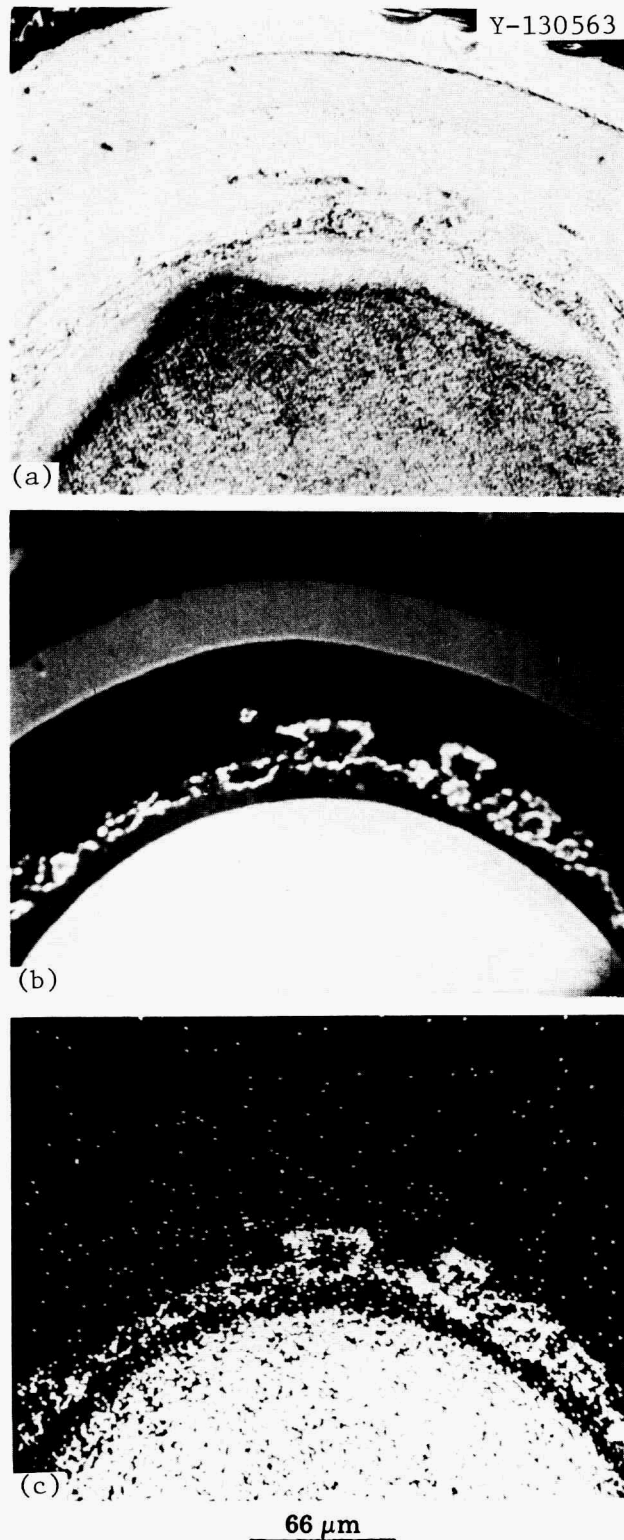


Fig. 5. Uranium Distribution in Coated, Carbonized, and Converted Weak-Acid Resin Microspheres. Batch A-615, 76.6%-converted. (a) Optical micrograph. (b) Backscattered electron image. (c) U $M\alpha$ x-ray image.

Y-128358

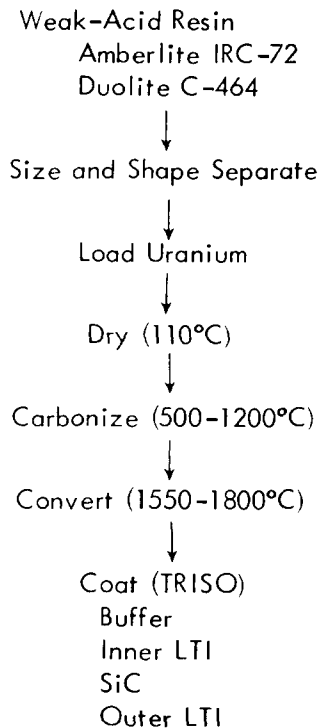


Fig. 6. Process Flowsheet for Preparation of Triso-Coated Resin-Derived Fissile Particles.

The conversion process may be interrupted at any intermediate point to produce a predetermined oxygen content or "conversion level." The current fuel design is based upon optimizing irradiation performance by suitably adjusting the conversion level. At the completion of the conversion process the average microspherule diameter is typically 360 μm , the density is approximately 3 g/cm^3 , and the uranium content by weight is approximately 75%. The partially converted material is shown by x-ray diffraction to be a mixture of UO_2 , UC_2 , and $\text{UC}_{1-x}\text{O}_x$. The concentration of each phase depends upon the conversion level and specific conversion conditions.

The converted spherical kernels are then Triso-coated as follows. A low-density (1.0–1.2 g/cm^3) buffer coating is deposited from acetylene, a high-density (1.85–2.0 g/cm^3) isotropic coating (LTI) from propylene or MAPP² gas, a SiC layer with near-theoretical density from methyltrichlorosilane (CH_3SiCl_3) and hydrogen, and finally an outer LTI PyC coating. A very thin PyC seal coat is often applied to the interface between the buffer and inner LTI to facilitate physical separation of the buffer and inner LTI for density determination. An impregnation seal coat is often applied to the inner LTI to SiC interface to reduce SiC penetration of the LTI.

²MAPP gas is marketed by AIRCO, Inc., and consists primarily of methylacetylene and propadiene with alkanes as stabilizers.

All kernel processing and coating are currently done in a vertical graphite resistance fluidizing furnace represented in Fig. 7. The particles are fluidized, typically in argon, for heat treatment or coating in a conical tube mounted in this furnace. Temperature is measured with optical pyrometry at and above 800°C and by a bed thermocouple below that temperature.

ORNL-DWG 75-3494

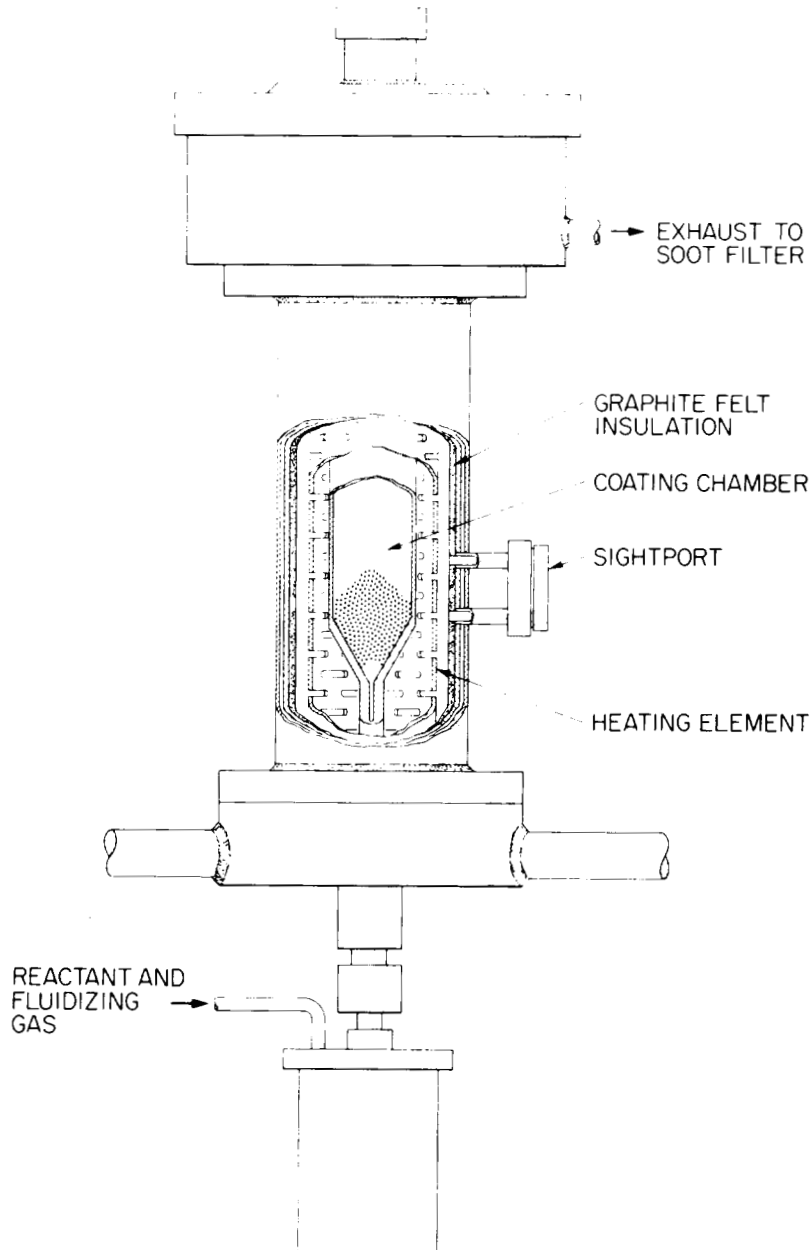


Fig. 7. Carbonization, Conversion, and Particle Coating Furnace.

After each processing step the batch weight, volume, and density are determined, and particle dimensions and quality are monitored by x radiography.

POSSIBLE CAUSES OF DISPERSION

To identify the cause(s) of the fuel dispersion phenomenon the following potential sources of uranium dispersion into the buffer were considered for study:

1. the presence of the nonequilibrium $UC_{1-x}O_x$ phase,
2. exposure of the kernels to air and/or moisture at critical process steps,
3. introduction of chlorine or fluorine at some process stage,
4. mechanical transfer of uranium-bearing particulates due to attrition during carbonization and/or conversion with subsequent incorporation of the particulates into the coating.

CLASSIFICATION OF DISPERSION TYPES

Since the amount and distribution of dispersed uranium varied widely, it was necessary to develop a consistent format for describing the state of fuel dispersion occurring in different situations. Six different cases of dispersion were delineated based upon the extent and location of the dispersed phase. These cases are shown in Fig. 8. The individual cases are described below:

- A. gross fuel dispersion, continuous throughout the buffer;
- B. gross fuel dispersion, discontinuous throughout the buffer;
- C. isolated globular regions of fuel dispersed in the buffer, with these regions not physically attached to the kernel;
- D. kernel surface roughening, with irregularities attached physically to the kernel;
- D'. fuel dispersion continuous around the kernel, with little radial penetration into the buffer;
- E. isolated thin halos or lenses of fuel dispersed in the buffer coating.

Most cases of observed dispersion closely resemble one of these cases, so that comparative evaluation of different batches on the basis of a percentage with a given descriptive type is possible. In determining a "dispersion rating," 100 to 200 particles were examined at random on the radiograph of a given particle type. Each particle was given a class grading from one of these six classes if it evidenced dispersion or "none" if no dispersion was resolvable when the radiograph was examined at 60 \times . Steward³ has determined that the limit of heavy metal radiographically detectable in fuel particles is approximately 1 wt % relative to the PyC. The classifications were sufficiently distinct to essentially eliminate

³K. P. Steward, *Methods for Determining Coating Contamination and Its Distribution in Nuclear Fuel Particles*, GA-9608 (August 1969).

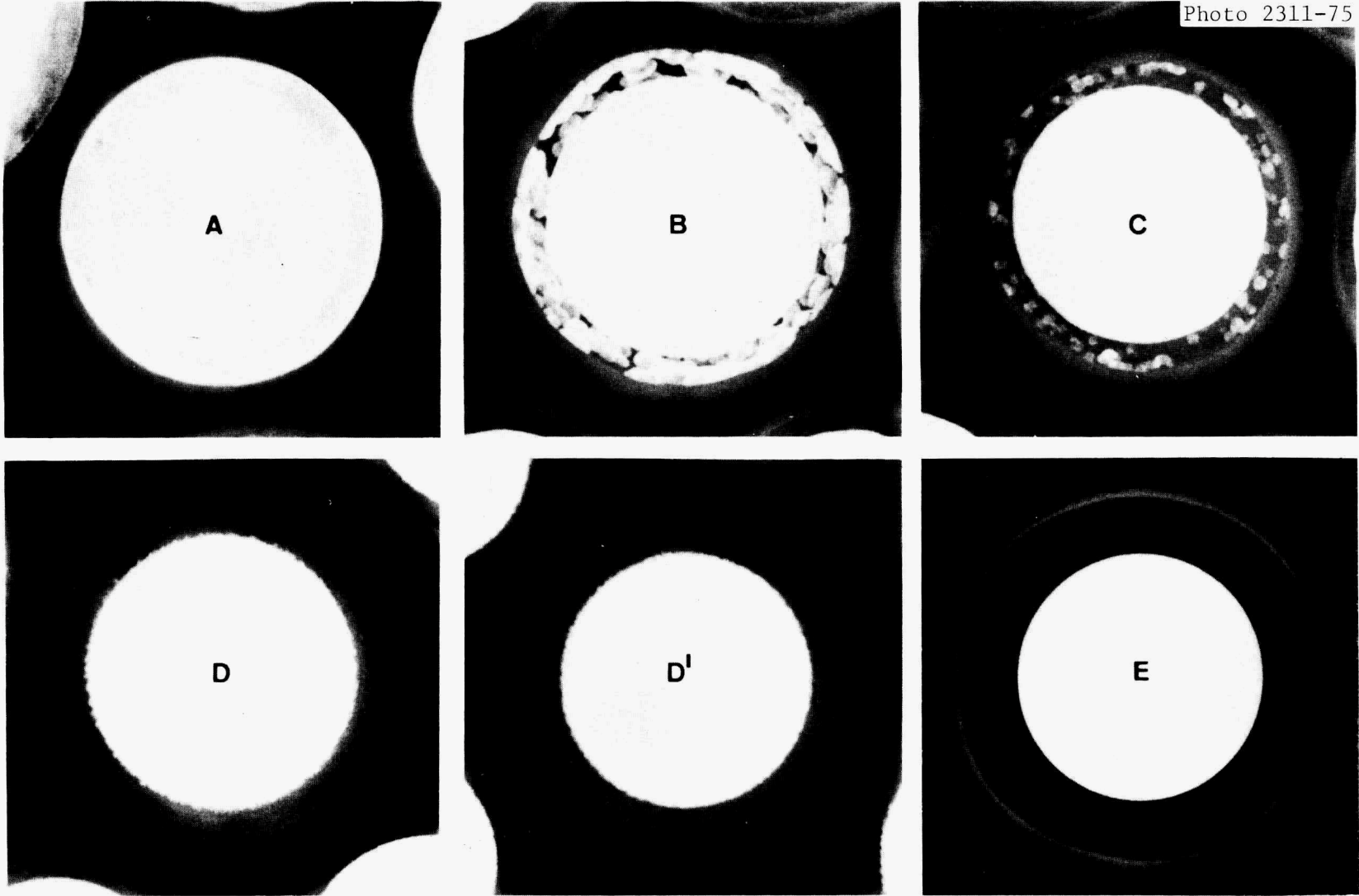


Fig. 8. Classification Types of Fuel Dispersion. 100×.

intermediate types, so that a rating for a given batch is considered to be representative of its behavior. The classification values are reported here as the percent of particles of a given type as 76A, indicating that 76% of the particles examined displayed gross fuel dispersion continuous throughout the buffer. The typical case for a small coater (≤ 0.06 m diam) facility, such as Fig. 1, indicated 100% "none" behavior. Certain large-coater (0.13 m diam) furnace runs such as Fig. 2, however, yielded the classifications shown in Table 1.

Table 1. Fuel Dispersion Results for 0.13-m-diam Coating Furnace

Batch	A	B	C	D	D'	E	None
J-505	8	0	28	36	26	0	3
A-608 ^a	7	4	2	20	0	1	66
A-602 ^a	50	11	7	20	0	6	6

^aAnnealing time was 30 min at 1800°C instead of the typical 60 min used in the remainder of this study. Dispersion values stated for this sample are thus somewhat low in comparison with other batches in the study.

EXPERIMENTS AND RESULTS

Effect of $UC_{1-x}O_x$ Phase on Fuel Dispersion

The effect of different kernel chemistry at equivalent conversion levels was examined. At a nominal 60 to 75% conversion level, the composition in some combination of UO_2 , UC_2 , and $UC_{1-x}O_x$ phases dispersed in excess carbon. The process of converting the UO_2 to the other phases in a fluidized bed involves removal of CO and a resultant dependence on the partial pressure of carbon monoxide at the conversion conditions. Therefore, by varying the conversion temperature or the partial pressure of CO in the fluidizing gas stream by adding CO, the proportion of phases produced for equivalent oxygen contents can be varied.

As the $UC_{1-x}O_x$ phase observed during normal conversion conditions is probably an intermediate phase, variation of temperature, time, or partial pressure of carbon monoxide over the bed should control the amount of $UC_{1-x}O_x$ present in the fuel kernel. Additionally, the introduction of small amounts of hydrogen into the fluidizing gas stream might serve to improve the carbon transport kinetics and thereby decrease the amount of $UC_{1-x}O_x$ present by permitting a closer approach to equilibrium.⁴ To

⁴J.F.A. Hennecke and H. L. Scherff, "Carbon Monoxide Equilibrium Pressures and Phase Relations During the Carbothermic Reduction of Uranium Dioxide," *J. Nucl. Mater.* 38: 285 (1971).

investigate these possibilities, runs were made to conversion levels of approximately 50% in argon at 1625 and 1505°C and at 1625°C in Ar-4% H₂ and Ar-6% CO, the CO content being 75% of the equilibrium P_{CO} .

The material was then ground in an inert-atmosphere glove box to -325 mesh and loaded in 0.5-mm-diam glass capillaries. Debye-Scherrer x-ray powder films were then made of these samples to qualitatively determine the phase composition. The conversion level was determined by chemical analyses.

The results are shown in Table 2 in order of decreasing amount of UC_{1-x}O_x phase. Run 238 had no detectable UC_{1-x}O_x phase. Runs 239 and 248 had essentially the same x-ray diffraction line intensities for this phase, which was in all instances a minor phase.

Table 2. Effect of Conversion Conditions on Amount of UC_{1-x}O_x Phase^a

Run	Temperature (°C)	Fluidizing Gas	Conversion (%)
234	1625	Ar	59
2369 HT 2	1625	Ar; exposed to air for 15 sec before and after conversion	57
248	1625	Ar-4% H ₂	42
239	1505	Ar	37
238	1625	Ar-6% CO (0.75 of the equilibrium P_{CO})	64

^aListed in order of decreasing amount, judged qualitatively from x-ray diffraction intensities.

It is apparent that increasing the conversion time by a factor of 4.5 while decreasing the temperature by 120°C results in less of the UC_{1-x}O_x phase being present in the kernels. Also, the addition of 0.75 of the equilibrium P_{CO} to quadruple the time at a given temperature for an equivalent conversion level essentially eliminated the UC_{1-x}O_x phase from the converted kernels. The use of a 4% H₂ addition decreased the amount of UC_{1-x}O_x approximately as much as does lowering the conversion temperature 120°C. The exposure of the carbonized resin to air before conversion does not appreciably affect the amount of this phase.

As run 234 is comparable with the conversion conditions normally used in fuel processing, minor amounts of UC_{1-x}O_x are probably present in most partially converted weak-acid resin fuels.

These kernels were then Bisoc coated by standard procedures in a small coater and annealed for 60 min at 1800°C. As about 30 min at 1800°C was required to produce observable fuel dispersion, a time of 60 min was used as a screening parameter. Material from runs 234, 238, 239, and 248 showed no radiographic evidence of fuel dispersion and was classified

as 100% "none" behavior, which is exemplified in Fig. 1. Run 2369 HT 2, which had been exposed to air, did, however, show a few irregularities on the surface of some kernels classified as 51% D and 49% D' behavior, as shown in Fig. 9.

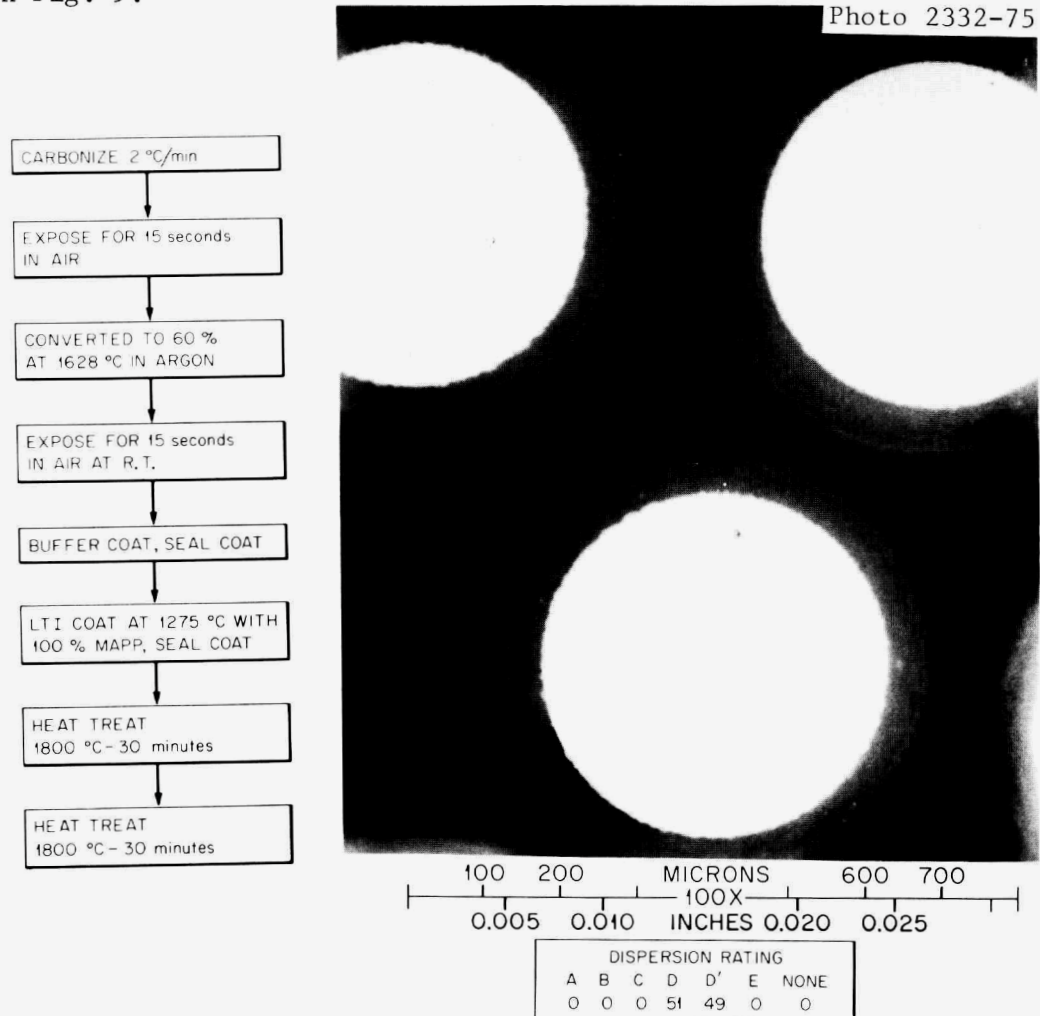


Fig. 9. Processing Steps and Radiograph of Air-Exposed, 60%-Converted Material. (OR-2369 HT-2).

Effect of Air and/or Moisture Exposure on Fuel Dispersion

Considerable evidence indicated that the high available surface area (BET $\approx 150 \text{ m}^2/\text{g}$) in these kernels and the reactive nature of finely dispersed uranium phases would lead to rapid oxidation and reaction if exposed to oxygen or water vapor.

Since exposure of the converted kernels to air and to water vapor before coating application could produce different dispersion effects as could the point in the process cycle where contamination occurred, these variables were combined in an attempt to isolate atmospheric contamination problems. These runs involved various combinations of exposure for 15 sec

to atmosphere (EA) and fluidizing a cold particle bed with water-saturated argon for 5 min [ArW]. Runs were also made continuously (no intermediate handling) from carbonization to final heat treatment to serve as controls. Unless otherwise noted, samples were converted at 1625°C in argon, Biso coated, heat-treated for 1 hr, and radiographed. The results are shown in Table 3 in approximate order of increasing severity of fuel dispersion. The ranking of runs in Table 3 is only qualitative because of the subjective nature of the comparisons and the relatively small differences between the extremes.

Table 3. Effect of Atmospheric Contamination on Fuel Dispersion

Run	Approximate Conversion (%)	Run Conditions	Extent of Fuel Dispersion
2377 H	70	Continuous run from carbonized material	Very few irregularities around some kernels
2386 H	77	Exposed in Ar storage box for 3.5 days	Very few irregularities around some kernels
2384 H	55	Continuous run from raw loaded resin	Irregularities around some kernels
2369 HT-2	57	EA ^a - convert - EA	Irregularities around some kernels
2375 H	70	EA - ArW ^b - convert	Irregularities around some kernels
2379 H	70	Convert - EA - ArW	Irregularities around most kernels
2382 H	70	Convert - ArW	Irregularities around most kernels
2380 H-2	55	Convert - ArW	Irregularities around many kernels; 20% of particles with a visible concentration of uranium in the buffer
2365 HT-2	55	Continuous run from raw resin	Irregularities around most kernels; most particles showing a uranium spot in buffer
2390 H	75 (1675°C)	Convert - ArW (20 min)	All particles showed irregularities, 6% showed slight uranium displacement into buffer

^aEA - exposed to air for 15 sec at room temperature.

^bArW - exposed to water-saturated argon for 5 min at room temperature.

The processing flow sheets and dispersion ratings for OR-2369 HT-2, -2375 H, -2379 H, -2386 HT, and -2390 H, which are representative of the behavior of the fuel when contaminated during handling, are shown in Figs. 9, 10, 11, 12, and 13, respectively. Continuous processing steps are depicted by individual boxes in the flowsheets.

Photo 2312-75

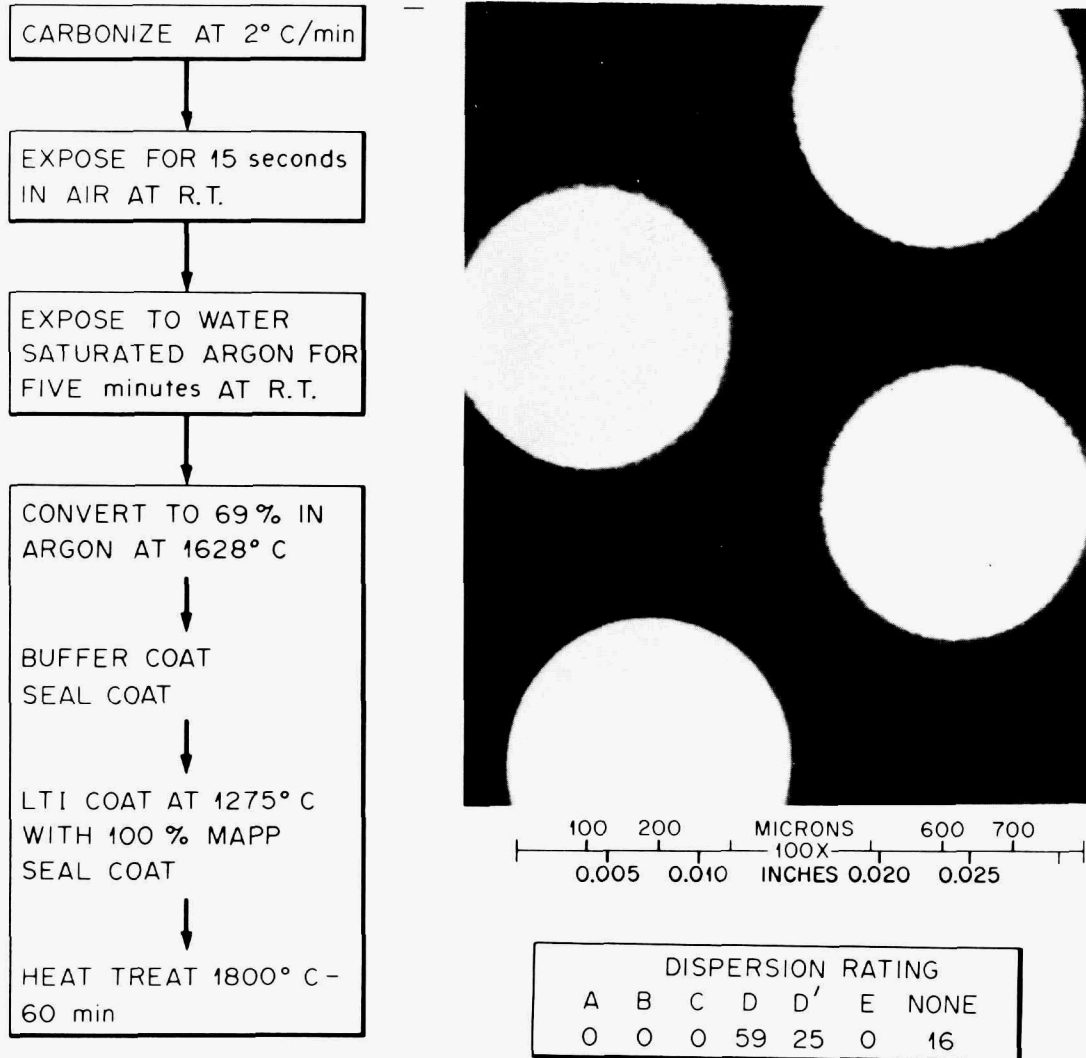


Fig. 10. Processing Steps and Radiograph of Air- and Water-Exposed, 69%-Converted Material. (OR-2375 H).

Photo 2333-75

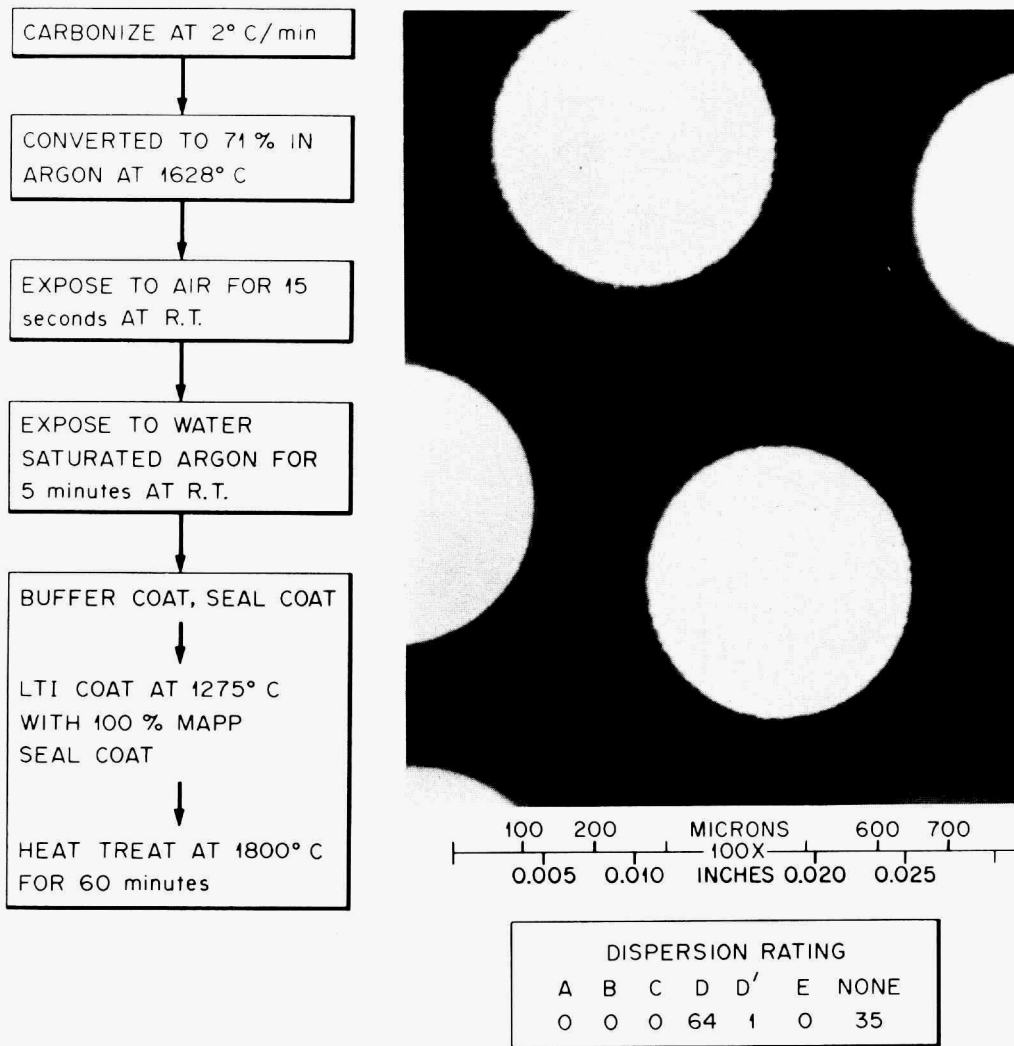


Fig. 11. Processing Steps and Radiograph of Air- and Water-Exposed, 71%-Converted Material. (OR-2379 H).

Photo 2329-75

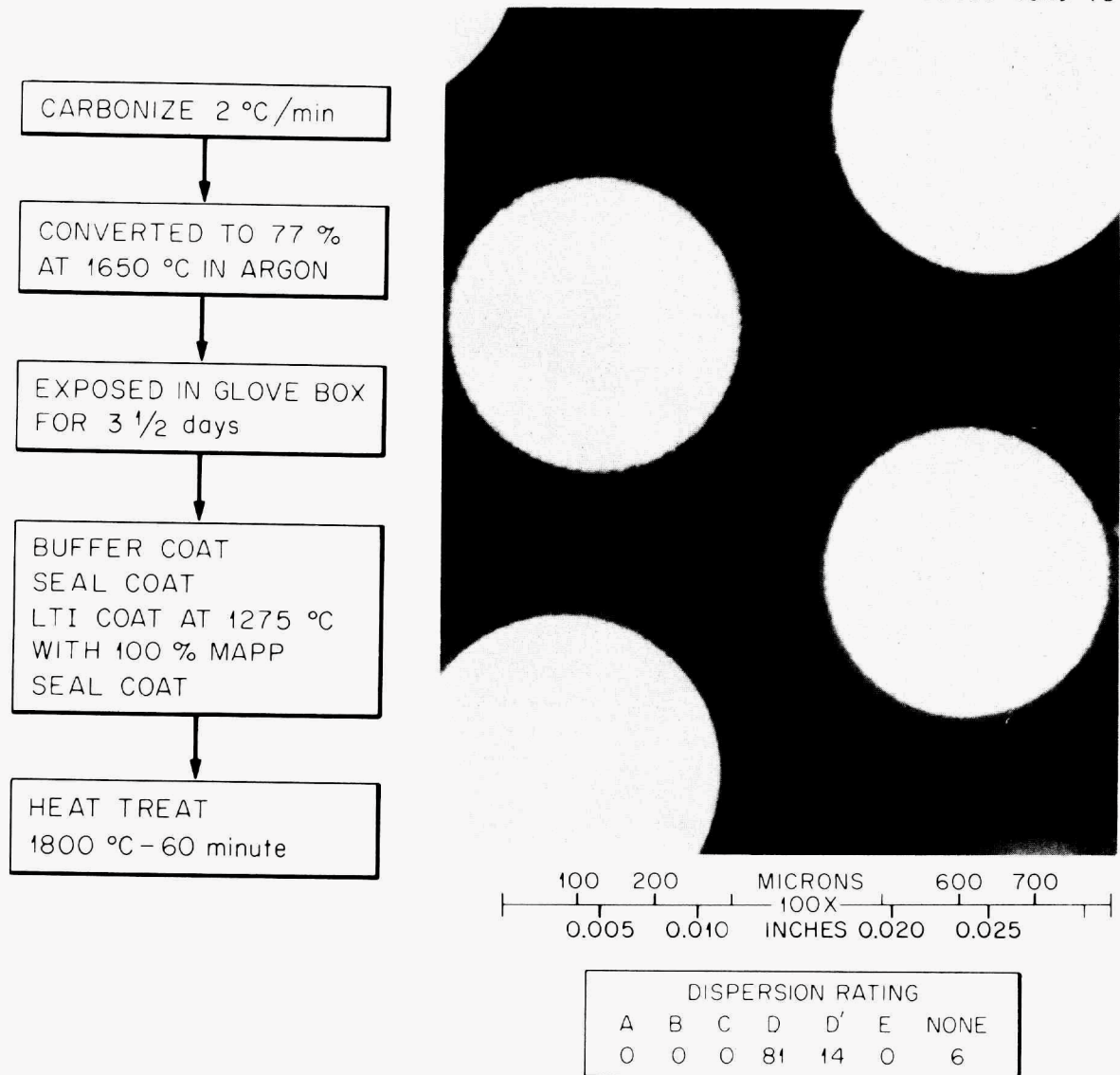


Fig. 12. Processing Steps and Radiograph of Glove-Box-Atmosphere-Exposed, 77%-Converted Material. (OR-2386 H).

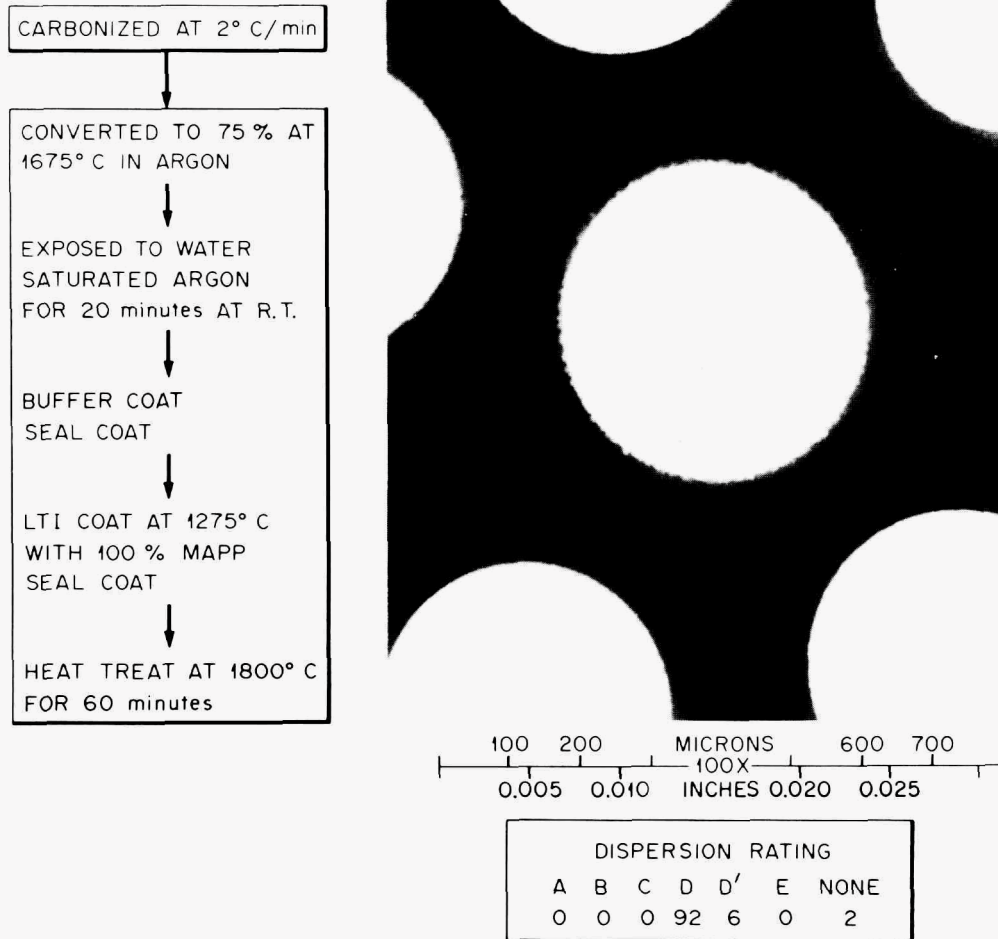


Fig. 13. Processing Steps and Radiograph of Water-Exposed, 75%-Converted Material. (OR-2390 H).

Effect of Chlorine Contamination on Fuel Dispersion

The volatilization of uranium from reaction of UO_2 and UC_2 with chlorine at elevated temperatures has been widely demonstrated in chlorine leaching of graphite.^{5,6} To investigate if chlorine could be the cause of fuel dispersion, several different possibilities were examined. The

⁵J. L. Cook and R. L. Hamner, *The Removal of Uranium and Thorium from Fueled-Graphite Materials by Chlorination*, ORNL-3586 (April 1964).

⁶D. E. LaValle, D. A. Costanzo, and W. J. Lackey, Jr., "The Determination of Particle Failure Fraction in HTGR Fuels," *Nuclear Technology* (in press).

- possible means by which chlorine could be introduced to the fuel include:
1. chlorine contamination of the source material,
 2. chlorine introduction into the coating process by residual chlorine or some other means,
 3. permeation of the LTI coating by chlorine during SiC deposition from the decomposition of methyltrichlorosilane (CH_3SiCl_3).

Chlorine Introduction During Coating

The off-gas flow from the 0.13-m prototype coating furnace in which fuel dispersion had been frequently produced is scrubbed with perchloroethylene (C_2Cl_4) to remove soot and tars from the effluent gas. The scrubbing tower is connected to the coating chamber with a large-diameter straight line. Because of the low flow velocities in the off-gas line, backstreaming of the C_2Cl_4 into the coating furnace was felt to be possible. To test this hypothesis an in-line container that would introduce C_2Cl_4 vapor to the coater gas was set up in the small coater during critical process steps.

Since fuel dispersion was apparently occurring from the kernel out into the buffer, and the LTI did not reveal any uranium by microradiographs, the C_2Cl_4 was applied during the buffer, seal, and LTI coating. As the fluidizing gas stream was swept across the surface of the C_2Cl_4 and its vapor pressure is slightly less than that of water, the fluidizing gas stream would presumably contain 2% or less C_2Cl_4 vapor.

A run made of 65%-converted material is shown in Fig. 14. Massive dispersion was produced, with 41% A and 59% B behavior. To examine the effect of conversion level on dispersion produced by C_2Cl_4 , kernels were prepared having approximately 10 and 100% conversion. The results are shown in Figs. 15 and 16, respectively. Continued heat treatment at 1800°C for an additional 60 min for the 10%-converted material considerably aggravated the fuel dispersion, as shown in Fig. 17. The dispersion rating for this material was approximately equal to the worst observed (i.e., that of the 100% converted material).

The effect of eliminating the $\text{UC}_{1-x}\text{O}_x$ phase was evaluated with a similar C_2Cl_4 run shown in Fig. 18. The fuel dispersion observed is more extensive than that shown in Fig. 14 for material of similar conversion level but having considerable amounts of $\text{UC}_{1-x}\text{O}_x$ present.

To further evaluate the importance of C_2Cl_4 backstreaming from the large coater off-gas scrubber, a run was made in which water was used in the scrubber in place of C_2Cl_4 . The result shown in Fig. 19, was minimal dispersion, showing that backstreaming of C_2Cl_4 enhanced dispersion of uranium in previous runs.

Permeation of the LTI Coating by Chlorine During SiC Deposition

The small coater line, which did not have a C_2Cl_4 off-gas scrubber, had during fabrication of material for HRB-9 and -10 irradiation tests produced fuel dispersion, as shown in Figs. 20, 21, and 22 for the

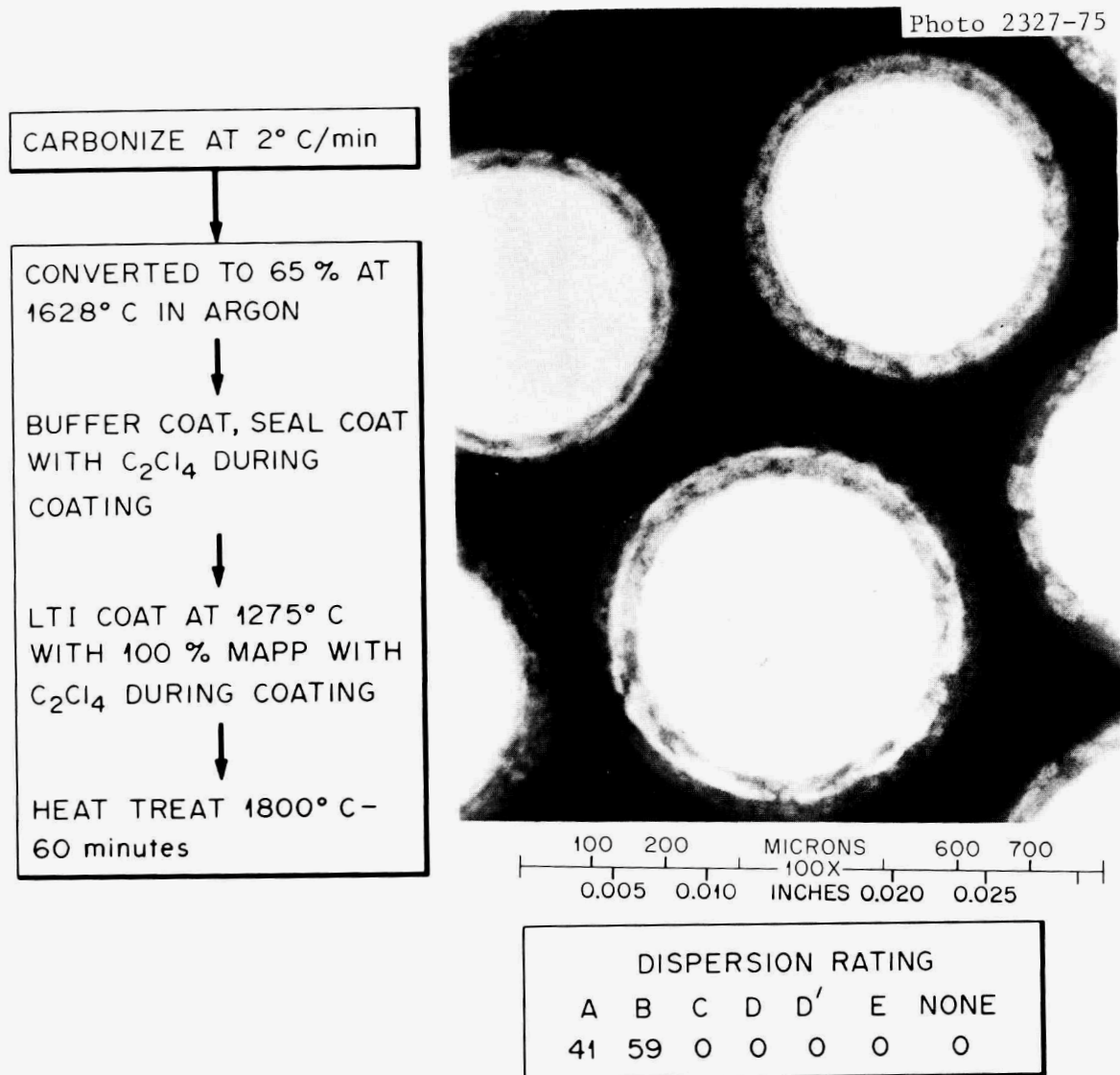


Fig. 14. Processing Steps and Radiograph of 65%-Converted Material Exposed to $\leq 2\%$ C₂Cl₄ During Coating. (OR-2407 H).

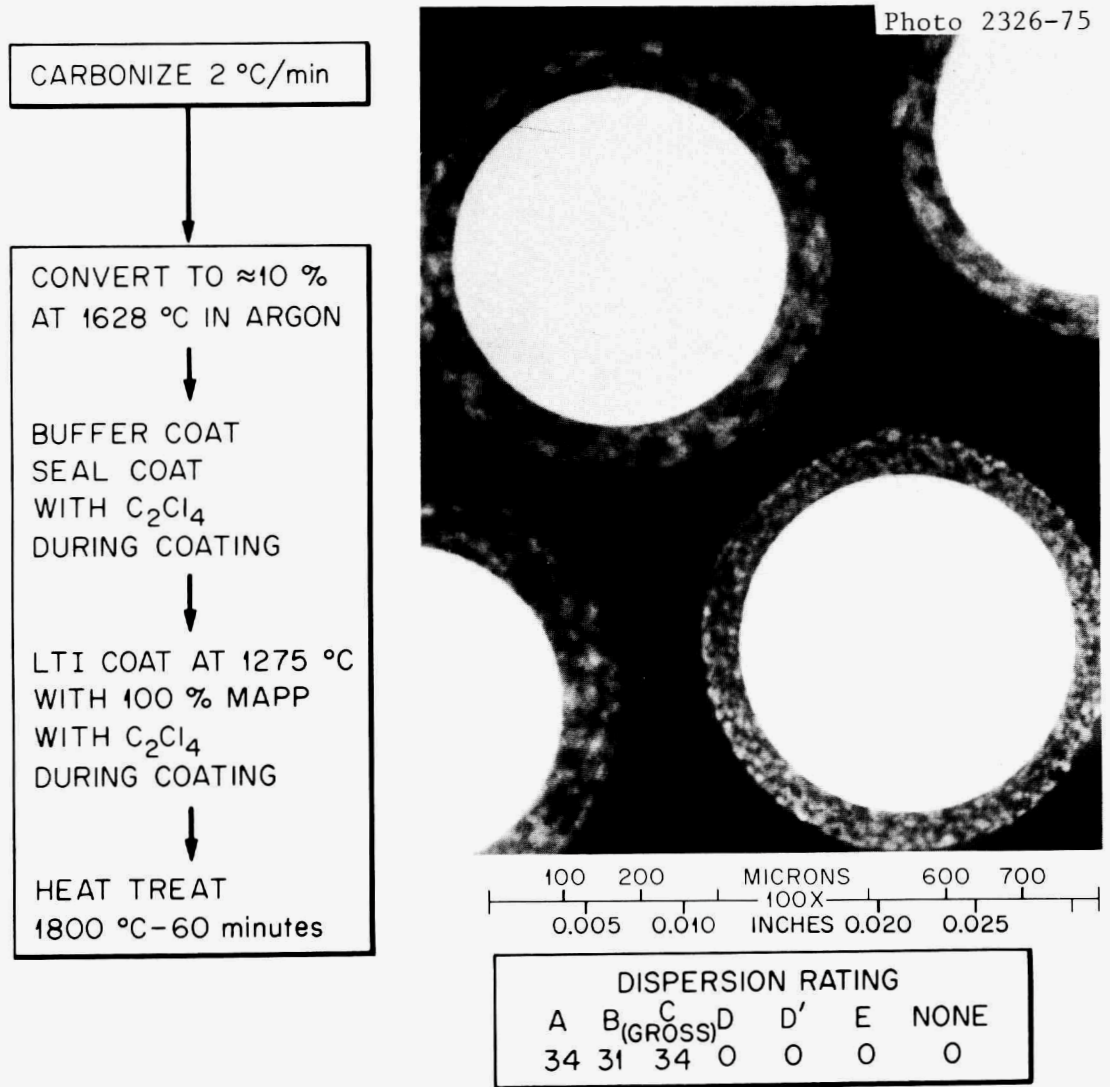


Fig. 15. Processing Steps and Radiograph of 10%-Converted Material Exposed to $\leq 2\%$ C₂Cl₄ During Coating. (OR-2419 AH).

Photo 2325-75

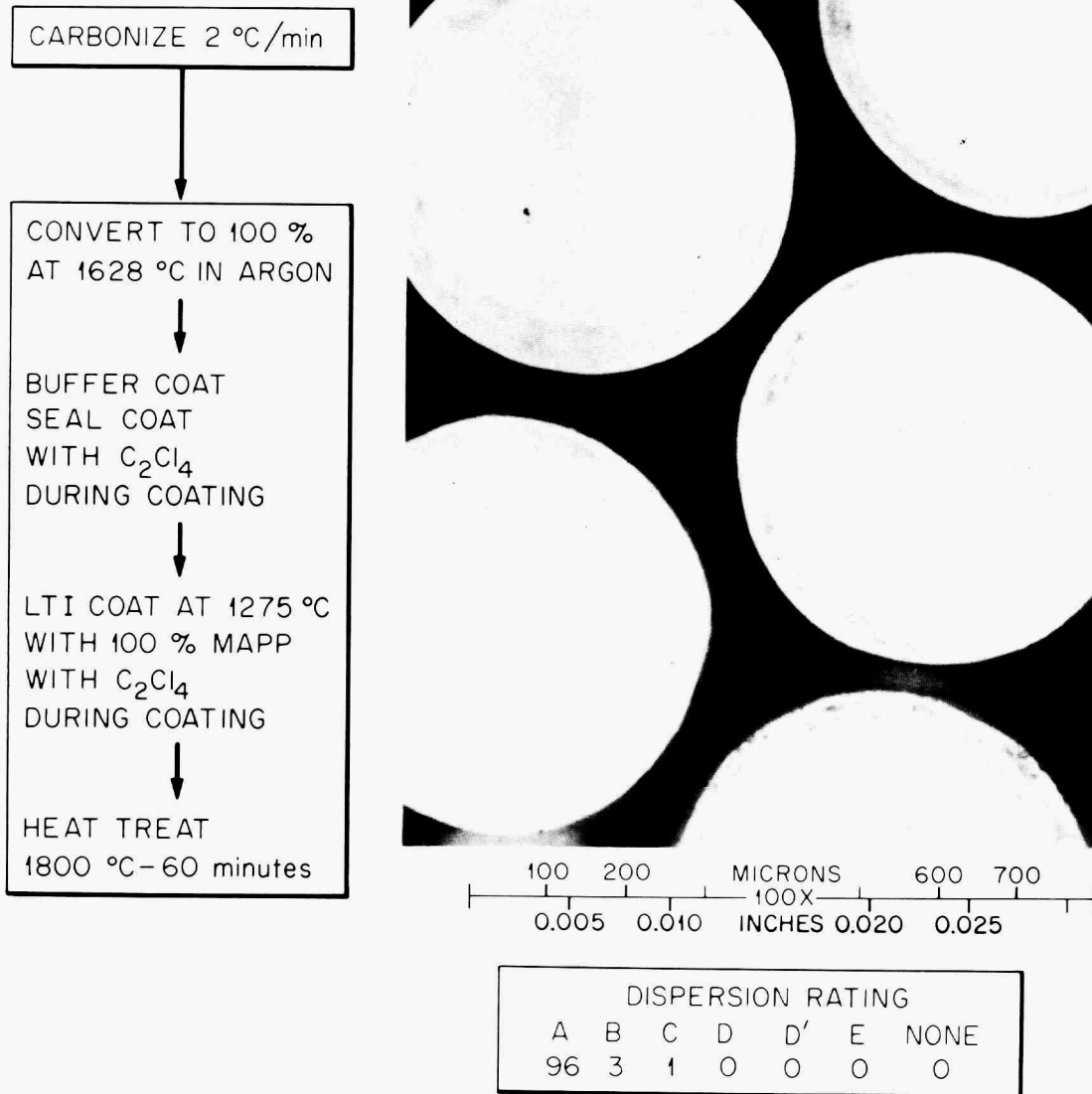
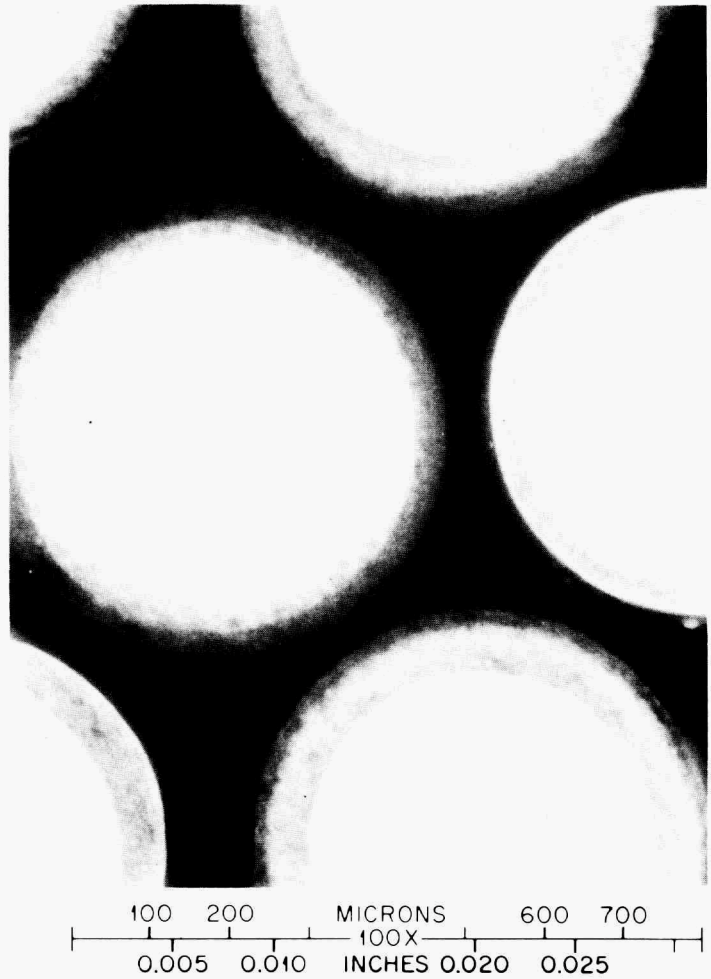
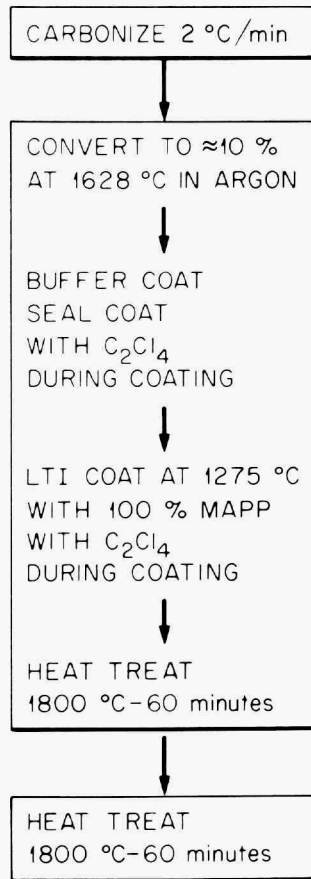


Fig. 16. Processing Steps and Radiograph of 100%-Converted Material Exposed to $\leq 2\%$ C₂Cl₄. (OR-2420 H).

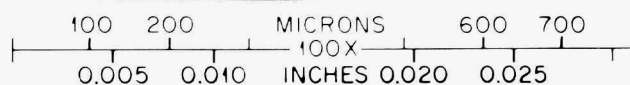
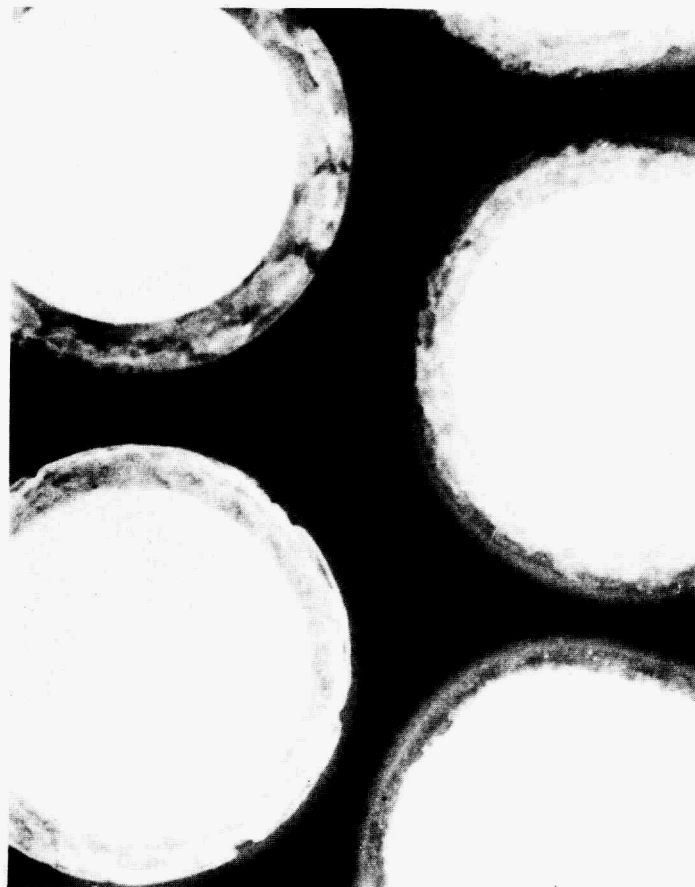
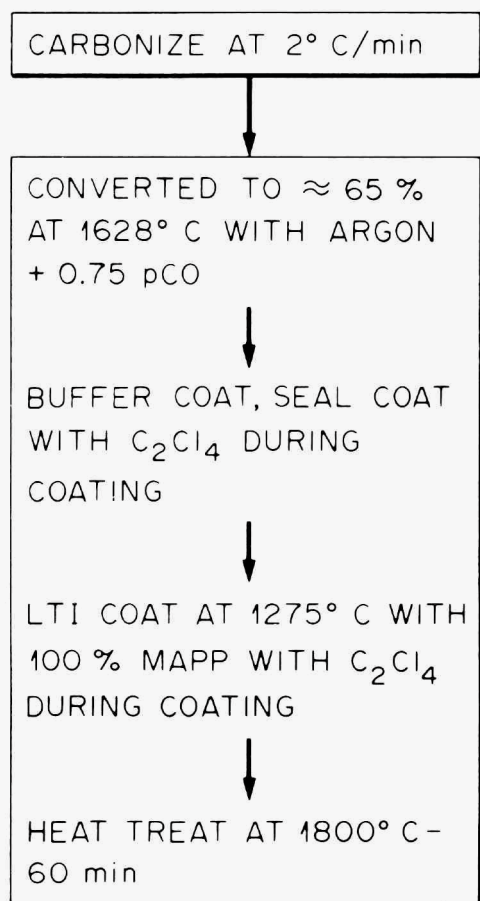
Photo 2324-75



DISPERSION RATING						
A	B	C	D	D'	E	NONE
94	6	0	0	0	0	0

Fig. 17. Processing Steps and Radiograph of 10%-Converted Material Exposed to $\leq 2\%$ C₂Cl₄ with Additional Annealing. (OR-2419 AH2).

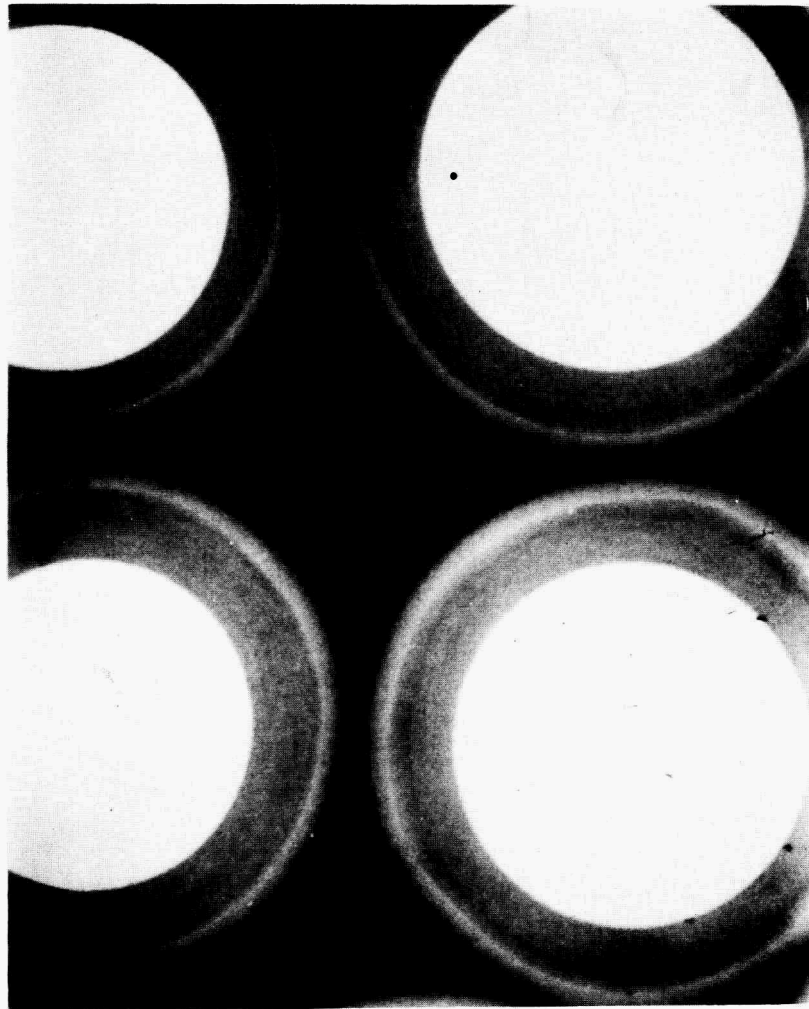
Photo 2323-75



DISPERSION RATING						
A	B	C	D	D'	E	NONE
81	18	1	0	0	0	0

Fig. 18. Processing Steps and Radiograph of 65%-Converted Material with no UC_xO_{1-x} Phase Exposed to ≤2% C₂Cl₄. (OR-2421 AH).

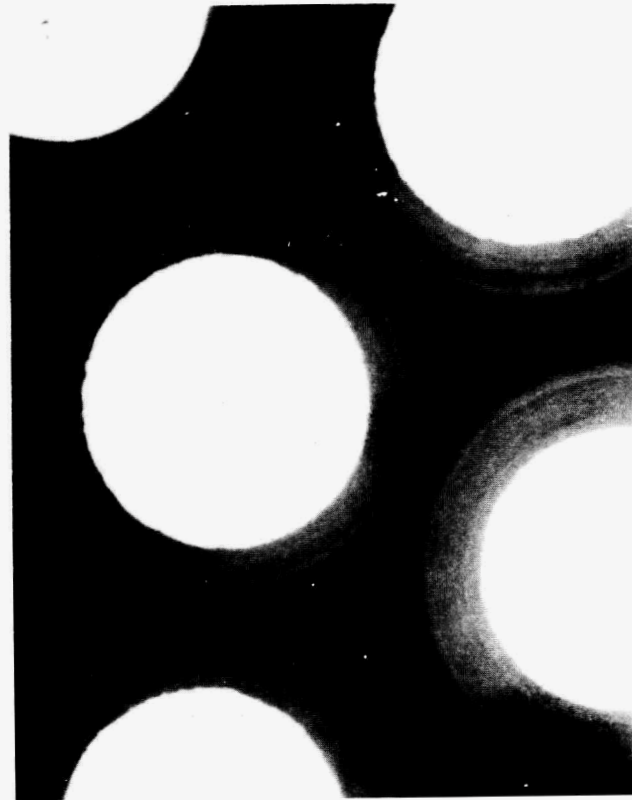
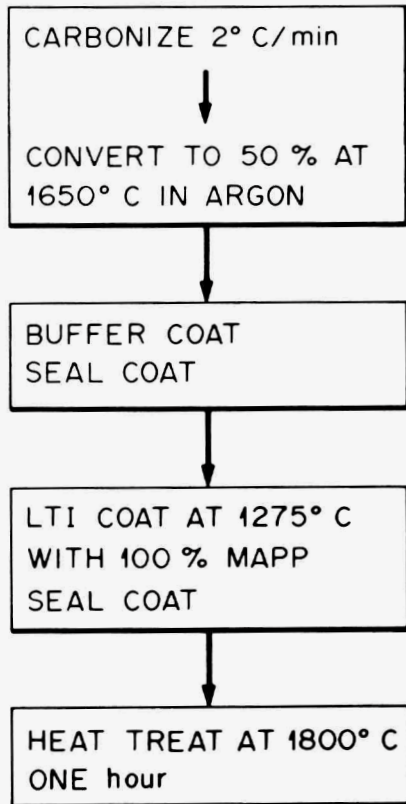
Photo 2322-75



DISPERSION RATING						
A	B	C	D	D'	E	NONE
0	0	0	2	0	0	98

Fig. 19. Appearance of 75%-Converted Material from 0.13-m-Diam Coater with Water Substituted for C_2Cl_4 in Off-Gas Scrubber. (A-360).

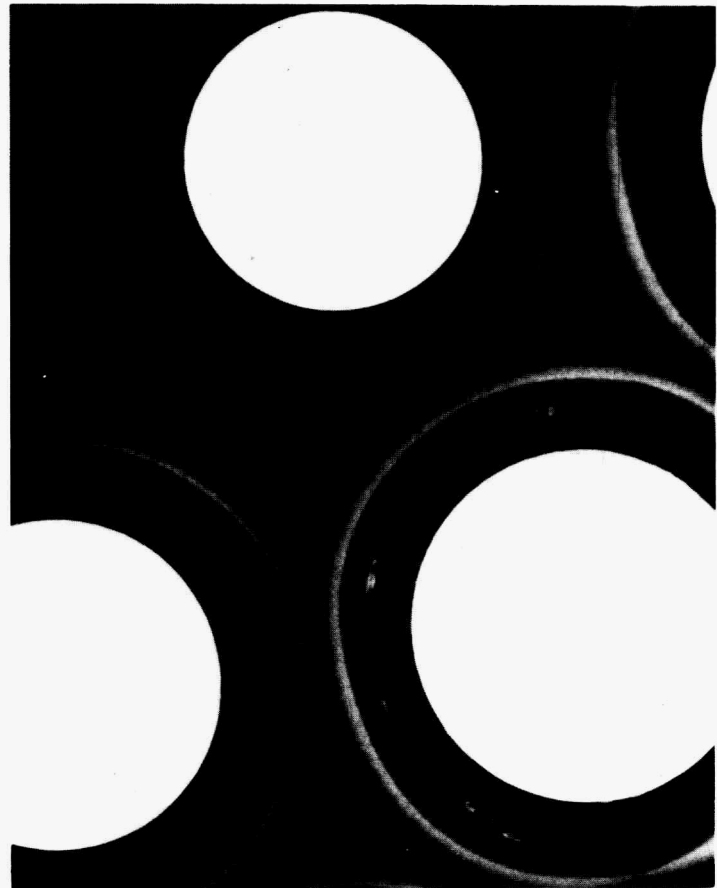
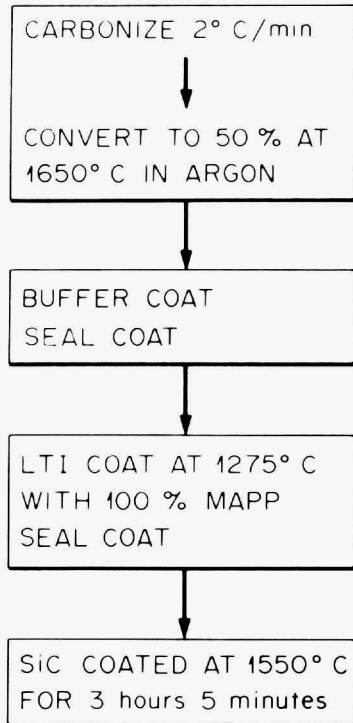
Photo 2321-75



DISPERSION RATING						
A	B	C	D	D'	E	NONE
0	0	1	56	26	0	16

Fig. 20. Processing Steps and Radiograph of 50%-Converted Material Produced in 64-mm-Diam Coater. (OR-2205 H).

Photo 2320-75



DISPERSION RATING						
A (FAINT)	B	C	D	D'	E	NONE
17	0	63	0	2	0	18

Fig. 21. Processing Steps and Radiograph of 50%-Converted Material with SiC Coating from 64-mm-Diam Furnace. (SC-236).

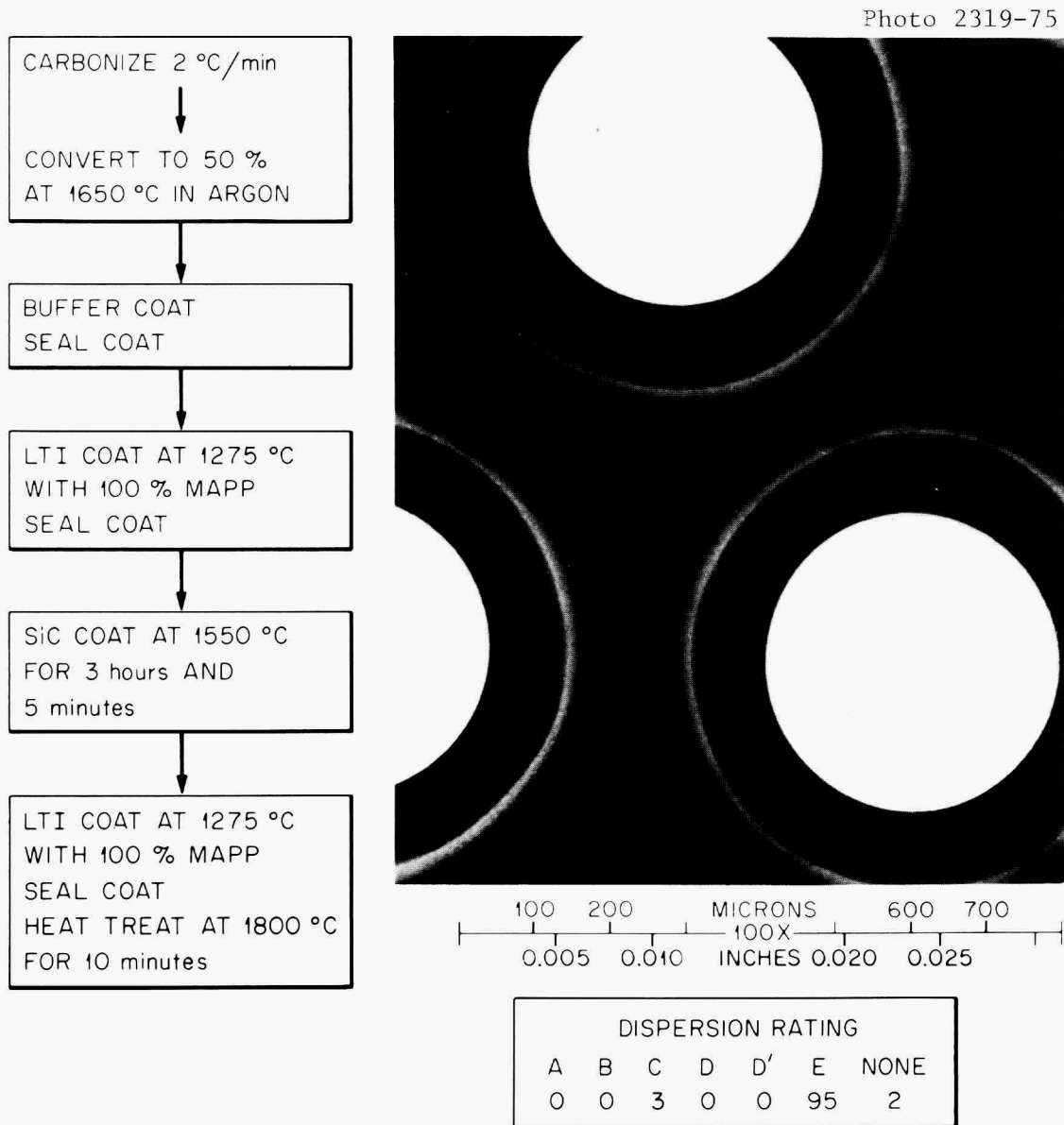


Fig. 22. Processing Steps and Radiograph of 50%-Converted Material with Triso Coating from 64-mm-Diam Furnace. (OR-2211 H).

Biso, SiC-coated, and Triso-coated particles, respectively. This series of runs was anomalous in that a water-cooled fluidizing gas injector was suspected of leaking water into the batch during conversion.

If chlorine is a factor in producing fuel dispersion in the absence of C_2Cl_4 , it is probably introduced by permeation of the inner LTI during SiC coating with methyltrichlorosilane. As the permeability of the LTI coating is a strong function of its density, changing the LTI density with all other test conditions held constant should affect the extent of fuel dispersion.

The density of LTI coatings decreases with increasing coating temperature, and open porosity increases with increasing reactant gas concentration. For example, an LTI applied at 1275°C with 10% MAPP coating gas would have a lower permeability than would a coating applied at 1325°C with 100% MAPP gas.

To test this hypothesis material was converted to nominal 65–75% levels in argon, exposed to water vapor during cooling from the conversion temperature, and also exposed to water vapor for 20 min at room temperature, buffer coated, and then given LTI coatings of different densities (and hence, permeabilities) before SiC coating. The SiC coating was deposited at 1550°C over a 3-hr period.

An example of an LTI coating deposited at 1275°C with 100% MAPP gas is shown in Fig. 23. A low-density, high-permeability coating was deposited at 1325°C with 100% MAPP gas (Fig. 24), and a high-density, low-permeability coating was produced with 10% MAPP gas at 1275°C (Fig. 25). It is apparent that fuel dispersion is more severe for higher LTI deposition temperatures and lower reactant gas dilutions.

We tried to produce fuel dispersion from the chlorine available during SiC coating without exposing the converted kernel to moisture. The highest permeability LTI coating of the set, which was produced at 1325°C with 100% MAPP gas, was used. The result is shown in Fig. 26. Again SiC coating was done for 3 hr at 1550°C.

Supportive experiments were also conducted to study the effects of LTI permeability on chlorine leachability in controlled analytical leach tests. The particles manufactured for this study were converted and buffer coated by standard techniques. The seal coats and LTIs were varied as described in Table 4. The chlorine leach tests were conducted at 1500°C for 2 hr on 5 to 15 g batches.⁷ X radiographs were made of selected samples after leaching. No visual evidence of damaged or cracked coatings was found in any of the experiments.

Chlorine leach tests were made for comparison of OR-2395 at three different temperatures for successive 2-hr anneals. The results are shown in Table 5. The radiographs for the particles that had been leached for 6 hr at the respective temperatures are shown in Fig. 27.

⁷D. E. LaValle, D. A. Costanzo, and W. J. Lackey, Jr., "The Determination of Particle Failure Fraction in HTGR Fuels," *Nuclear Technology* (in press).

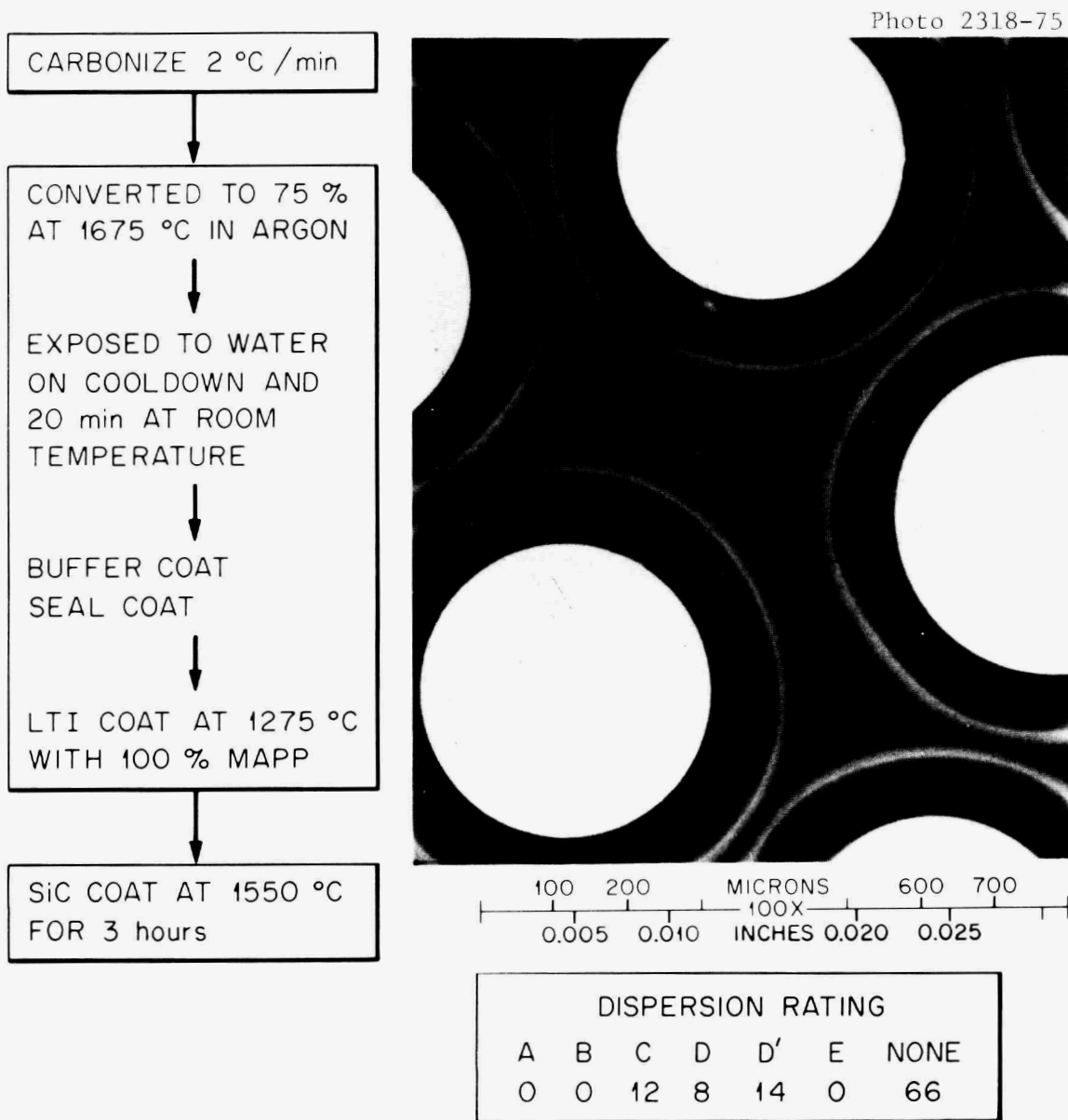


Fig. 23. Processing Steps and Radiograph of a Water-Exposed, 75%-Converted Material with a Typical Process LTI and SiC Coating. (SC-321).

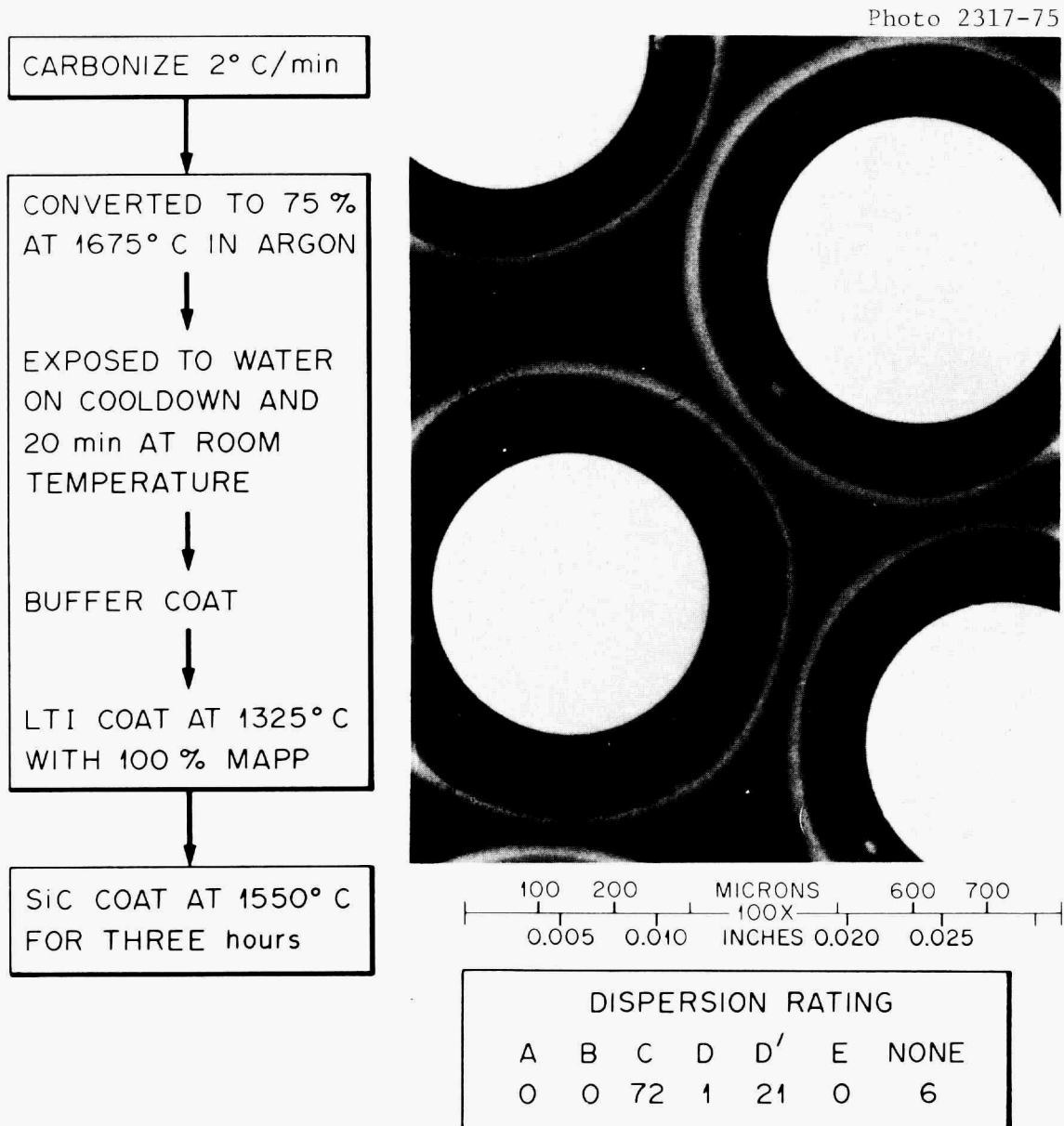
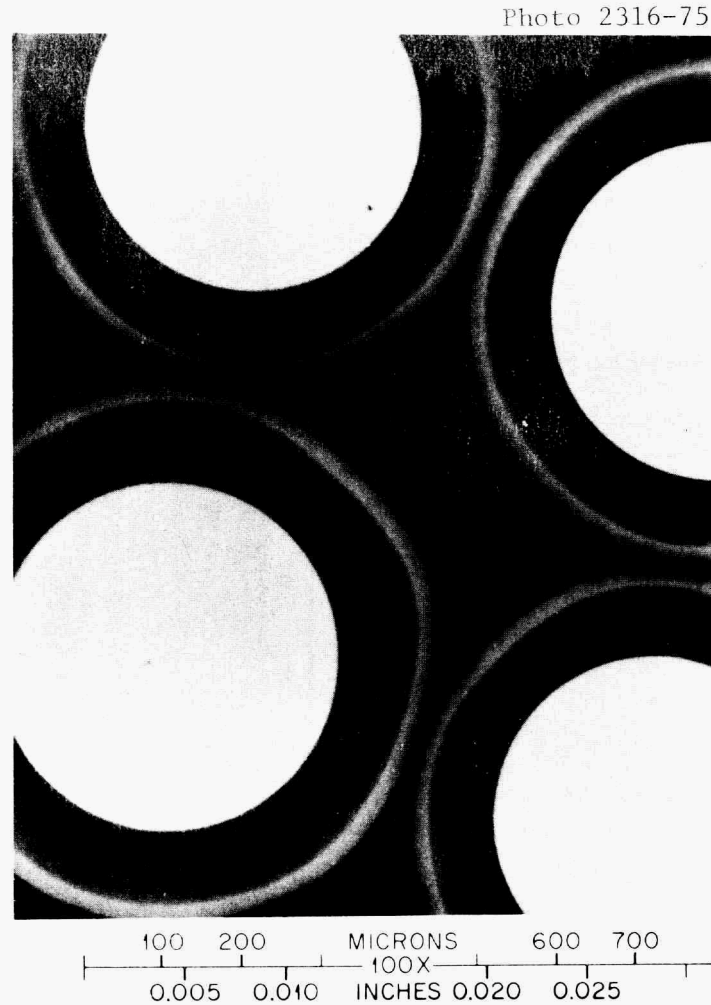
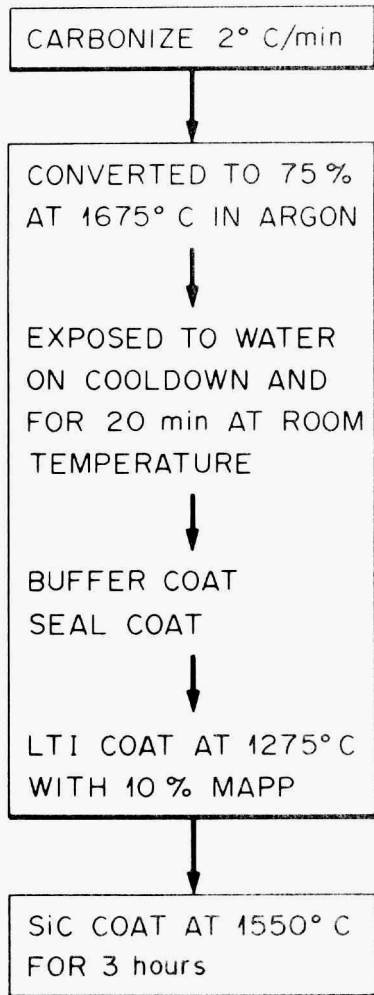


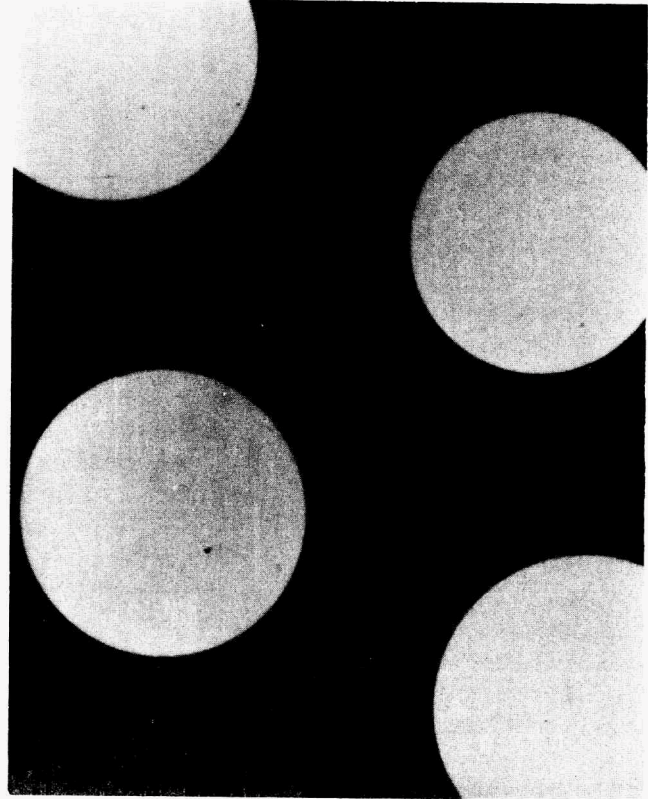
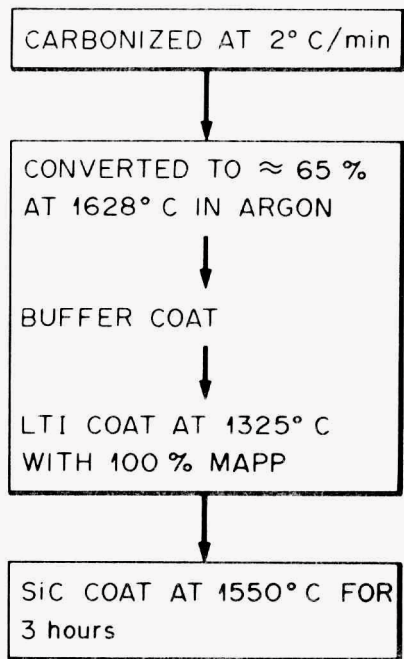
Fig. 24. Processing Steps and Radiograph of Water-Exposed, 75%-Converted Material with a High-Permeability LTI and Typical SiC Coating. (SC-322).



DISPERSION RATING						
A	B	C	D (FAINT)	D'	E	NONE
0	0	0	3	0	0	97

Fig. 25. Processing Steps and Radiograph of Water-Exposed, 75%-Converted Material with a Low-Permeability LTI and Typical SiC Coating. (SC-323).

Photo 2315-75



DISPERSION RATING						
A	B	C	D	D'	E	NONE
0	0.5	46	0	7	0	47

Fig. 26. Processing Steps and Radiograph of 65%-Converted Material with a High-Permeability LTI Coating without Kernel Exposure with an SiC Coating. (SC-324).

Table 4. Chlorine Leach Results for Different PyC LTI Coatings Deposited on WAR Kernels

Batch	LTI Thickness ^a (μm)	Density ^b (g/cm^3)	Deposition Temperature ($^{\circ}\text{C}$)	MAPP Gas Concentration (%)	Kernel Conversion Level (%)	Fraction of U _{removed} ^c
OR-2395	36.7 [3.4]	1.952	1275	100	25	10.2×10^{-4} 3.2 8.9 44.7
OR-2395-HT ^d	36.7 [3.4]	1.952	1275	100	25	17.4
OR-2395-S ^e	41.0 [1.9]	1.985	1275	100	25	16.3
OR-2395-S HT	41.0 [1.9]	1.985	1275	100	25	17.4
OR-2396	32.7 [1.7]	1.959	1275	100	25	14.9
OR-2396-S	31.5 [1.9]	1.941	1275	100	25	15.0
OR-2397	54.3 [3.3]	1.962	1275	100	25	12.6
OR-2397-S	58.4 [3.2]	1.953	1275	100	25	17.9
OR-2398	41.1 [2.2]	1.939	1275	100	25	44.0
OR-2398-S	42.6 [2.2]	1.948	1275	100	25	29.4
OR-2399	43.9 [2.9]	1.877	1350	100	25	1040.0 766.7
OR-2399-S	46.8 [3.4]	1.883	1350	100	25	118.7
OR-2400	39.2 [2.3]	1.914	1275	50	25	0.6 3.3 4.3
OR-2400 HT	39.2 [2.3]	1.914	1275	50	25	8.9
OR-2400-S	40.6 [2.9]	1.922	1275	50	25	4.8
OR-2401	38.7 [1.8]	1.844	1325	50	25	7.2 3.0 3.0
OR-2401 HT	38.7 [1.8]	1.844	1325	50	25	10.8
OR-2401-S	44.7 [2.5]	1.857	1325	50	25	2.3
OR-2427	36.4 [3.0]	1.918	1275	75	25	13.3 6.4
OR-2429	36.7 [4.1]	1.846	1325	75	25	162.3 335.5
OR-2343	39.2 [4.3]	1.955	1275	100	0	1.2
OR-2344 (S)	43.1 [3.5]	1.955	1275	100	0	0.5
OR-2346	39.5 [2.8]	1.958	1275	100	50	2.0
OR-2347	40.8 [3.7]	1.964	1275	100	50	1.6

^aNumber in brackets is standard deviation for 30 particles.

^bObserved gradient density.

^cChlorine leach was done at 1500 $^{\circ}\text{C}$ for 2 hr.

^dHT designates heat treatment at 1800 $^{\circ}\text{C}$ for 30 min.

^e"S" designates seal coat.

Table 5. Chlorine Leach Results as a Function of Time and Temperature

Temperature ($^{\circ}\text{C}$)	Fraction of Uranium Removed		
	First 2 hr	Second 2 hr	Third 2 hr
1000	1.30×10^{-4}	0.7×10^{-4}	0.5×10^{-4}
1250	2.0	1.8	4.3
1500	3.2	8.0	154.4

Photo 2314-75

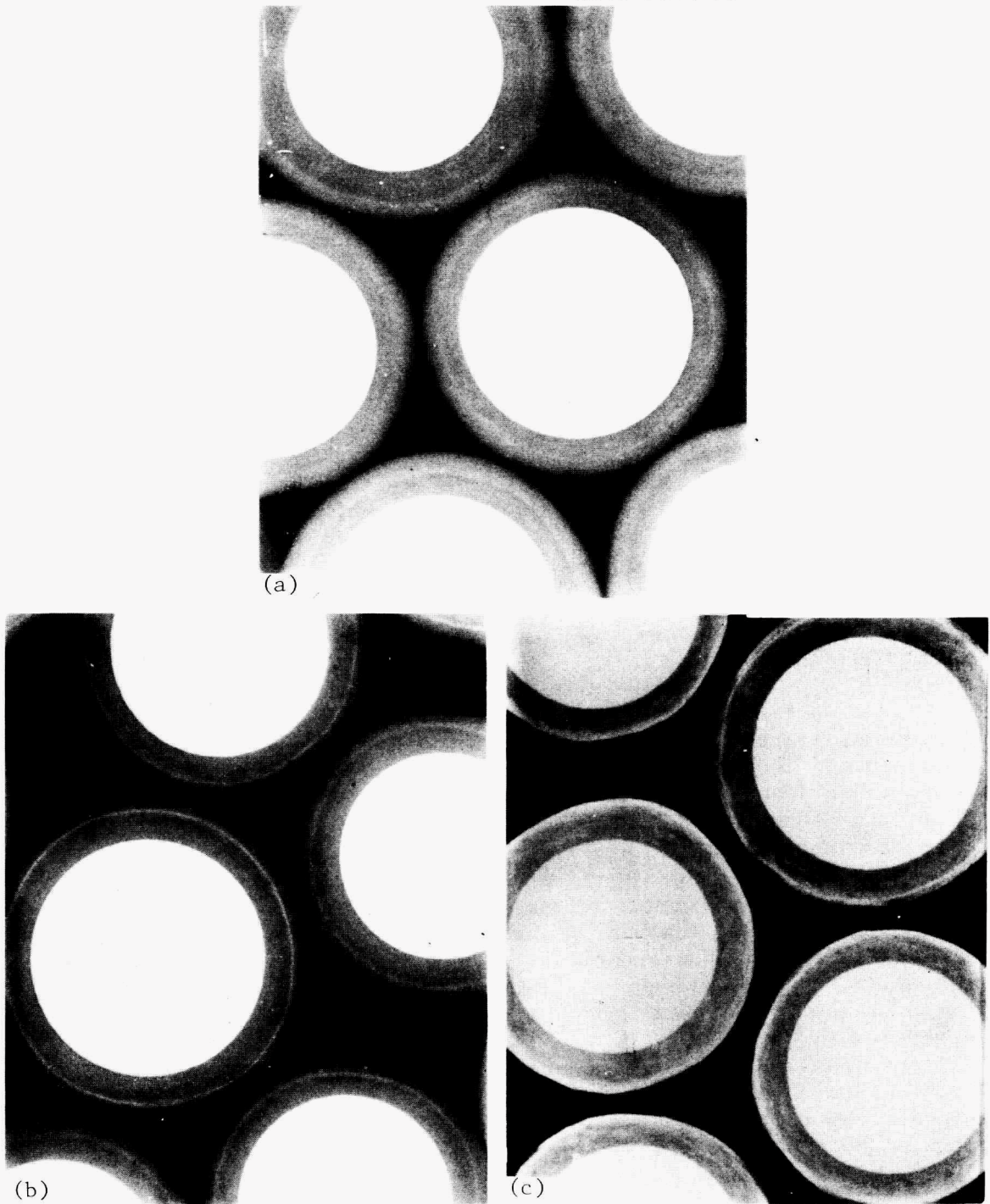


Fig. 27. Particles of OR-2395 Chlorine Leached for 6 hr at the Indicated Temperatures, Demonstrating the Presence of Uranium in the Buffer. (a) 1000°C, (b) 1250°C, and (c) 1500°C. 84×.

Mechanical Attrition

A further potential source of uranium contamination of the buffer region is mechanical attrition of the kernels before coating. The fluidization of the bed during conversion of weak-acid resin particles with low mechanical strength could conceivably produce fine particles containing uranium, which may subsequently be deposited onto the buffer. These fines would be expected to ride considerably above the normal fluidized bed height. After buffer coating, the fines that had been well above the bed may become mechanically attached to the porous buffer when the run is terminated. These fines would then be incorporated at the buffer/LTI interface by subsequent LTI coating. This particulate transfer would not produce extensive fuel dispersion but would be a potential source of occasional fuel fragments at the buffer/LTI interface.

A run in which the entire converted batch (presumably including any fines) was buffer coated is shown in Fig. 28(a). The appearance is very similar to that described as type C fuel dispersion. The x-ray sample holder used was then cleaned, protective sheeting was replaced, and the sample was radiographed again. The result, shown in Fig. 28(b), indicates that a substantial quantity of fines had been removed from the buffer surface.

DISCUSSION OF RESULTS

The comparison of behavior of kernels with different $UC_{1-x}O_x$ concentrations indicated that considerable variation in the amount of this phase is possible. The normal conversion conditions of 1625°C in argon produce considerable amounts of $UC_{1-x}O_x$. This phase can be essentially eliminated if 0.75 times the equilibrium carbon monoxide pressure over the UO_2 - UC_2 -C system is introduced into the fluidizing gas stream during conversion. Also, lowering the conversion temperature 120°C or adding approximately 4% H_2 to the fluidizing gas stream decreased the amount of the $UC_{1-x}O_x$ phase considerably. However, in two such runs (234 and 238) having markedly different concentrations of the $UC_{1-x}O_x$ phase in the kernels, neither showed any evidence of fuel dispersion. This indicated that the $UC_{1-x}O_x$ phase was not, of and by itself, a determining factor in fuel dispersion.

The observation that exposure to air for 15 sec before and after conversion (Run 2369 HT-2) produced irregularities around kernels indicated several supportive experiments. However, although many different combinations of moisture and oxygen exposure were used both before and after conversion, it was not possible to produce extensive fuel dispersion by atmospheric contamination alone. The clear indication from these data on various handling conditions is that simple atmospheric contamination caused by exposure during handling contributes very little to fuel dispersion. The 15-sec open-air exposure represents a worst-case situation. At the end of this 15-sec period the particles were becoming discolored and were generating considerable heat from oxidation. The kernels are, however,

Photo 2313-75

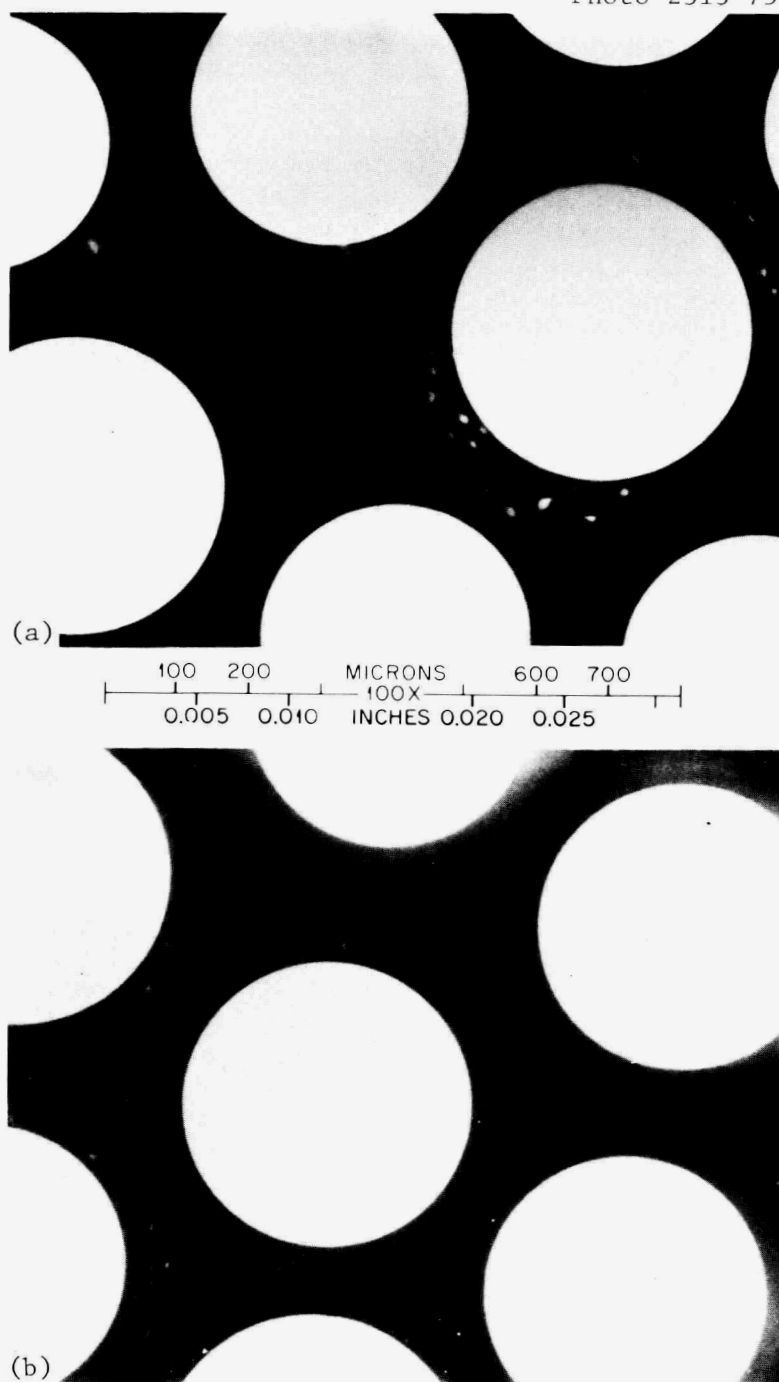


Fig. 28. Nominally Converted Material for which Entire Converted Batch was Used in Buffer Coating. (a) As coated. (b) With cleaned sample holder and protective film.

slightly more prone to exhibit fuel dispersion if contaminated after conversion than before. This is apparent from the observations of fuel dispersion as well as from the comparative heating behavior of the particles on exposure to an oxidizing atmosphere before and after conversion.

Exposure of fuel kernels to water vapor after conversion produced more extensive fuel dispersion than did air exposure. However, even in the worst cases, when using the small coater we could not duplicate the extensive fuel dispersion found in particles from the 0.13-m prototype coater furnace depicted in Fig. 2. As the exposures to air and/or moisture were considerably worse than what might be expected during normal process handling, it is very unlikely that handling or storage exposure alone is capable of subsequently causing extensive fuel dispersion.

We could not explain the apparently anomalous behavior of the dispersion occurring in Run 2365 HT-2 for kernels produced in a continuous run from raw resin. Identical conditions used in the continuous Run 2384 H produced very little evidence of dispersion.

Introduction of C_2Cl_4 into the fluidizing gas stream during buffer and LTI coating produced massive and extensive fuel dispersion in the buffer region. As C_2Cl_4 is used in the off-gas scrubber from the large coater furnace, it was strongly indicated that back-streaming of C_2Cl_4 was responsible for the massive dispersion observed in the prototype coater fuel. Different conversion levels run in this manner clearly demonstrated that the severity of fuel dispersion increases with increasing conversion level. This behavior is in accordance with previous work, which indicated that UC_2 is more susceptible to chlorine leaching than is UO_2 .

Heat treatment for an additional 60 min at $1800^\circ C$ considerably aggravated the fuel dispersion. Elimination of the $UC_{1-x}O_x$ phase aggravated fuel dispersion when the batch was exposed to C_2Cl_4 during coating. As $UC_{1-x}O_x$ is formed at the expense of UC_2 , the indication is that the $UC_{1-x}O_x$ is less leachable than is UC_2 . Runs made in the prototype coater furnace when water was substituted for C_2Cl_4 produced no fuel dispersion. It thus seems clear that the gross fuel dispersion found in particles prepared in the prototype coater was due to C_2Cl_4 back-streaming from the off-gas scrubber.

This did not, however, explain all fuel dispersion that had been observed. The smaller coater furnace, which did not have a C_2Cl_4 off-gas scrubber, had, on one occasion, produced serious fuel dispersion. This run was anomalous in that a water-cooled fluidizing gas injector was suspected of leaking water into the batch. The extent of fuel dispersion did not approach that shown in Fig. 2 but was approximately that produced by exposing the batch to water-saturated argon and/or air. This served to confirm the hypothesis that a leaking gas injector may have hydrolyzed this batch. Subsequent silicon carbide coating had then produced extensive fuel dispersion. As CH_3SiCl_3 is used in the deposition of silicon carbide coatings, a ready source of chlorine is available in the fluidizing gas stream during this process step. The implication was that the hydrolyzed uranium-bearing kernel had increased susceptibility to chlorine leaching from the chlorine available during SiC coating. If this were the case, the permeability of the inner LTI to chlorine during SiC deposition should be a controlling factor in determining the extent

of fuel dispersion. Coating chlorination studies showed that LTI permeability is a direct function of density and of reactant gas concentrations, so that varying LTI deposition conditions should control or eliminate fuel dispersion occurring during SiC deposition.

When LTI coatings with different permeabilities were applied to kernels that had been exposed to water, very different degrees of fuel dispersion were produced when an SiC coating was applied. We observed no gross fuel dispersion of A or B types as for the material exposed to C_2Cl_4 . The higher density (lower permeability) coatings displayed less fuel dispersion. The coatings made with 10% MAPP gas at $1275^\circ C$ had excellent resistance to chlorine permeation and hence allowed little fuel dispersion. However, PyC deposited under these conditions has poor irradiation stability. Thus, optimum LTI deposition conditions must be a compromise minimizing permeability while decreasing coating gas concentration to a level consistent with good irradiation stability. The results on exposure of the kernels to moisture followed by low-density LTI and SiC coating confirm the behavior in the anomalous small coater run and explain the remaining observed case of fuel dispersion.

The transport of uranium into the buffer region of a SiC-coated Biso particle that had not been exposed to moisture demonstrates the importance of LTI density. The high permeability (low density) LTI coating was applied at $1325^\circ C$ with 100% MAPP gas. This run showed a considerable number (46%) of the particles with regions of high uranium concentration in the buffer region and 7% with slight haloing of the kernel. A previous run, which was identical except for exposure to moisture for 20 min at room temperature, displayed regions of high uranium concentration in the buffer in 72% of the particles examined and 21% with haloing of the kernel. This indicates the considerable importance of moisture contamination in aggravating fuel dispersion in marginal conditions.

The run without moisture exposure strongly suggests that the current LTI coating process of $1275^\circ C$ with 100% MAPP may be marginal with regard to permeation of the LTI by chlorine. A significant deviation in LTI deposition temperature or exposure of the kernels to moisture during handling is capable of producing low-level fuel dispersion during SiC deposition. This fact is of considerable significance in the design of HTGR process flow sheets.

The chlorine leach results at $1500^\circ C$ for 2 hr identified the important parameters in defining LTI permeability. These data showed considerable variation in the fraction of uranium removed for identical samples. The clear indication is that standard LTI coatings on weak-acid resin kernels are permeable to some extent to chlorine at $1500^\circ C$. As the concentration of MAPP gas used for LTI coatings decreases, the coatings are less permeable. This effect has also been observed when propylene (C_3H_6) is used in the coating gas. The temperature sensitivity of the coating process decreases considerably as the MAPP concentration decreases. Therefore, dilution of the MAPP gas to 50% decreases the leachability and allows wider process variation for an acceptable product from a chlorine leach standpoint. The behavior of diluted MAPP gas coatings under irradiation is currently under investigation. Preliminary results indicate the 50% dilution levels produce coatings with good irradiation stability.

These chlorine leach data also tentatively suggest that an increase in inner LTI thickness from 32 to 55 μm has little significant effect on

the chlorine leachability. These data are not in agreement with information obtained on Biso-coated ThO_2 particles, which indicated that LTI thickness did significantly affect permeability.⁸ However, a strong dependence of uranium removal on LTI density is apparent. At the same coating gas concentration, a decrease in gradient column density from 1.92 to 1.88 g/cm^3 caused a 15-fold increase in the uranium removed.

Placing a seal coat on the outside of the inner LTI does not appear to have a clearly distinguishable effect on the amount of uranium removed by chlorine leaching. The large uncertainty in the reported values makes a clear evaluation of the effect currently impossible. Furthermore, annealing the particles for an additional 30 min at 1800°C does not have any significant observable effect on LTI permeability within the accuracy of the present method.

The conclusions to be drawn are that LTI density and coating gas dilution are very significant in controlling uranium leaching by chlorine at 1500°C, and that LTI thickness, annealing, and the presence of a seal coat have little effect in preventing fuel dispersion.

The chlorine leach tests made at 1000, 1250, and 1500°C showed that the amount of uranium removed increases markedly with increasing temperature. The nearly constant removal rates at 1000 and 1250°C indicate a continuous permeation of the LTI coating. The rate of uranium removal at 1500°C increases with time. The radiograph indicates a considerable quantity of uranium transferred to the buffer by chlorination, and uniformity from particle to particle. The radiograph of all the particles rules out the possibility that the uranium removed could result from a few cracked coatings.

Irradiation tests in the HFIR capsules HRB-9 and -10 on the fuel-dispersed material shown in Figs. 20, 21, and 22 indicate that fuel dispersion of this limited extent does not affect irradiation stability of the coatings. Particles displaying the gross fuel dispersion shown in Fig. 2 are currently being irradiated in the ORR capsule OF-2.

The indication from the single run in which some slight type C behavior was observed after buffer coating is that mechanical attrition can produce sufficient fines to give the appearance of limited fuel dispersion. Fines produced during conversion may also explain the anomalous behavior observed in one continuous run (2365 HT-2) that displayed some type C fuel dispersion. These fines would ride above the normal fluidized bed height but could easily be incorporated during coating as particles occasionally cycled well above the bed. During a continuous run from raw resin to Biso-coated particles there would be no opportunity to remove the fines so that they might be incorporated during coating. The quantity of fines produced during conversion may vary considerably but does not, in any event, constitute more than a very small fraction of the bulk material. Mechanical attrition does not appear to be able to produce other than occasional isolated minor and sporadic fuel dispersion. If fuel dispersion from this source were identified as a problem from the

⁸W. J. Lackey, Jr., J. D. Sease, D. A. Costanzo, and D. E. LaValle, "Improved Coating Process for High-Temperature Gas-Cooled Reactor Fuel," *Trans. Am. Nucl. Soc.* 22(TANSO 22): 194-95 (November 1975).

standpoint of irradiation performance, a rapid screening step after conversion to remove any fines would prevent their subsequent incorporation during coating. More extensive investigation of this phenomenon is necessary.

CONCLUSIONS AND RECOMMENDATIONS

The occurrence of fuel redistribution in the buffer region of Biso and Triso uranium-loaded weak-acid resin particles has been identified with two primary causes. The presence of perchloroethylene in off-gas scrubbing systems is believed to provide sufficient chlorine from backstreaming during coating to cause gross fuel dispersion. The chlorine available during SiC deposition with methyltrichlorosilane is capable of producing limited fuel dispersion if the LTI coating is sufficiently permeable. This is particularly acute if the fuel kernel has been previously exposed to moisture or oxygen. Simple handling and storage exposures and phase composition are not, by themselves, capable of producing fuel dispersion.

Chlorine leach results have shown that LTI permeability is a strong function of density, coating gas dilution, and coating temperature. Permeability of the LTI coating is relatively unaffected by LTI thickness, seal coat applications, and subsequent annealing of the LTI.

Mechanical attrition during conversion is capable of producing occasional low-level apparent fuel dispersion if fines are carried over during processing. Recommendations include the following.

1. Contact of weak-acid resin with perchloroethylene (or other source of chlorine) during processing must be avoided.
2. Permeability of the inner LTI must be sufficiently low to resist chlorine permeation during application of the SiC coating with methyltrichlorosilane. Increased density and coating gas dilution consistent with irradiation stability should be used to produce low-permeability LTI coatings.
3. Exposure of carbonized and converted weak-acid resin particles to oxygen and/or moisture must be minimized.
4. Mechanical attrition may introduce fines during conversion and could require mechanical separation before buffer coating.

ACKNOWLEDGMENTS

The carbonization, conversion, and carbon coating runs were very ably performed by C. Hamby, Jr. The SiC coatings were furnished by J. I. Federer and J. W. Geer. Uranium-loaded resin particles were supplied by P. A. Haas of Chemical Technology Division. We wish to acknowledge W. P. Eatherly for his assistance in planning the test program and T. B. Lindemer for many helpful suggestions. We are grateful for the cooperation of D. A. Costanzo and D. E. LaValle for the chlorine leaching operation, E. P. Griggs for metallography, and W. J. Mason for microradiography of samples. The authors also acknowledge the assistance of S. Peterson for technical editing and Regina Collins for typing and preparation of the report.

INTERNAL DISTRIBUTION

1-2.	Central Research Library	79-81.	W. J. Lackey, Jr.
3.	Document Reference Section	82.	T. B. Lindemer
4-13.	Laboratory Records Department	83.	E. L. Long, Jr.
14.	Laboratory Records, ORNL RC	84.	A. L. Lotts
15.	ORNL Patent Office	85.	A. P. Malinauskas
16.	G. M. Adamson, Jr.	86.	M. T. Morgan
17-19.	R. L. Beatty	87.	K. J. Notz
20.	E. S. Bomar	88.	A. R. Olsen
21.	R. A. Bradley	89.	W. H. Pechin
22.	A. J. Caputo	90.	C. B. Poillock (Y-12)
23.	J. A. Carpenter	91.	J M Robbins
24.	J. H. Coobs	92.	J. E. Rushton
25.	W. H. Cook	93.	J. L. Scott
26.	D. Costanzo	94.	J. D. Sease
27.	J. E. Cunningham	95.	J. H. Shaffer
28.	W. P. Eatherly	96.	D. P. Stinton
29.	J. I. Federer	97-99.	V. J. Tennery
30.	P. A. Haas	100.	T. N. Tiegs
31.	R. L. Hamner	101.	T. N. Washburn
32.	J. W. Hill	102-111.	G. W. Weber
33-35.	M. R. Hill	112.	J. R. Weir, Jr.
36.	F. J. Homan	113.	W. C. Leslie (consultant)
37.	D. R. Johnson	114.	John Moteff (consultant)
38.	M. J. Kania	115.	Hayne Palmour III (consultant)
39-76.	P. R. Kasten	116.	J. W. Prados (consultant)
77.	R. K. Kibbe	117.	G. V. Smith (consultant)
78.	H. P. Krautwasser	118.	D. F. Stein (consultant)

EXTERNAL DISTRIBUTION

119-120. USERDA DIVISION OF NUCLEAR FUEL CYCLE AND PRODUCTION, Washington, DC
20545

Director

121-122. USERDA DIVISION OF REACTOR RESEARCH AND DEVELOPMENT, Washington, DC
20545

Director

123--124. USERDA OAK RIDGE OPERATIONS OFFICE, P.O. Box E, Oak Ridge, TN
37830

Director, Reactor Division
Research and Technical Support Division

125--286. USERDA TECHNICAL INFORMATION CENTER, Office of Information Services,
P.O. Box 62, Oak Ridge, TN 37830

For distribution as shown in TID-4500 Distribution Category,
UC-77 (Gas-Cooled Reactor Technology)